Amphiphilic poly(vinyl alcohol) membranes leaving out chemical cross-linkers: Design, synthesis, and function of tailor-made poly(vinyl alcohol)-*b*-poly(styrene) copolymers

*Alessandro Angelini, Anja Car, Ionel Adrian Dinu, Luigi Leva and Wilfredo Yave**

This work is dedicated to our beloved mentor, friend, scientist, collaborator, and great person Prof. Wolfgang Meier. We will remember him for his energy, tenacity, and his positive thoughts. He was a brilliant and visionary scientist who gained worldwide scientific recognition for his work. Despite the hard illness, he stayed passionate about science until the last breath. “He will stay in our hearts”

A. Angelini, A. Car, I. A. Dinu
Department of Chemistry, University of Basel, Mattenstrasse 24a, BPR 1096, 4058 Basel, Switzerland

L. Leva, W. Yave
Research and Development Department, DeltaMem AG, Hegenheimermattweg 125, 4123 Allschwil, Switzerland
E-mail: wilfredo.yave@deltamem.ch

Keywords: poly(vinyl alcohol), block-copolymers, self-assembly, membranes, pervaporation

Tailor-made poly(vinyl alcohol)-*b*-poly(styrene) copolymers (PVA-*b*-PS) for separation membranes are synthesized by the combination of reversible-deactivation radical polymerization (RDRP) techniques. The special features of these di-block copolymers are the high molecular weight (>70kDa), the high PVA content (>80 wt.%) and the good film-forming property. They are soluble only in hot dimethyl sulfoxide (DMSO), but by the “solvent-switch” technique, they self-assemble in aqueous media to form micelles. When the self-assembled micelles are cast on a porous substrate, thin film membranes with higher water permeance than that of PVA homopolymer are obtained. Thus, by using these tailor-made PVA-*b*-PS copolymers, we demonstrate that chemical cross-linkers and acid catalysts would no longer be needed to produce PVA membranes, since the PS nanodomains within the PVA matrix act as cross-linking points. Lastly, subsequent thermal annealing of the thin film enhances the membrane selectivity due to the improved microphase separation.

1. Introduction

Design, synthesis, and use of new nanostructured materials are very important in today's world. According to the Sustainable Development Goals (SDG) from the United Nations (Goal 7), "energy is central to nearly every major challenge and opportunity the world faces today".[1] Therefore, innovation in material synthesis and material processing is a key and a driving force to achieve goals related to clean/sustainable energy and to energy efficient processes.

In the last twenty years, scientists focused on design and synthesis of new amphiphilic block copolymers with fascinating properties for nanolithography, photonics, photovoltaics, membranes, and drug delivery.[2-8] These copolymers are a family of polymers having two or more polymer chains (blocks) chemically bonded to each other, and they can self-assemble into ordered nanodomains due to their peculiar chemical and physical properties.[9-11] The control and manipulation of those nanostructured patterns by different methods has been intensively studied too.[10, 12-18] In fact, block copolymer thin films coated on a flat substrate have attracted attention because they are precursor materials for nanodevices and for synthetic membranes that are used in separation technologies. As membranes, they have been studied as nanostructured dense and porous membranes, they displayed stimuli-responsive properties and superior separation performance than those obtained from conventional polymers used in the membrane fabrication.[19-24] However, very often, the right block-copolymer as membrane material (with specific molecular weight and block ratio) does not exist or its synthesis is very difficult, and thus, the design and synthesis of tailor-made block-copolymers for separation membranes are still challenging within the scientific community.

Due to the polymer solution properties and as solid films, amphiphilic block copolymers based on poly(vinyl alcohol) and poly(styrene) (PVA-*b*-PS) could become important and attractive in the field of coatings, thin films, drug delivery and emulsion systems.[25-28] Both PVA and PS blocks as homopolymers are widely used in a range of industrial products, from packing, membranes, electronics and automotive to food, medical and pharmaceutical applications.[29-31] Although PVA-*b*-PS copolymers were already synthesized in the past following different methods of synthesis,[32-35] they have not attracted much attention compared to other block copolymers. This could have happened because high molecular weight copolymers with narrow molecular weight distribution and controlled PVA/PS block ratio are difficult to obtain. [34-42] The reported copolymers exhibit low molecular weights, and the ratio of PVA/PS are not suitable for applications where they could have a great potential, e.g., for membrane fabrication. So, obtaining block copolymers with high molecular weights

and controlled PVA block is a great challenge. Briefly, PVA-*b*-PS with molecular weights within the range of 2kDa to 60kDa has been reported. Although the PVA/PS ratio can be well controlled, the combination of PVA/PS ratio with the molecular weight of copolymer are not the appropriate as membrane material. To produce synthetic membranes, the copolymer must have good film-forming property. Thus, PVA-*b*-PS copolymers with the combination of molecular weight higher than 60kDa and PVA/PS ratio between 4 and 20 (wt.%/wt.%) are needed.

In the field of membranes, PVA homopolymer is industrially used to produce different types of membranes because it is one of the most hydrophilic polymers, as well as simple to process.[27, 30, 43, 44] In addition, PVA is a semicrystalline polymer with good mechanical and thermal properties.[44-46] Because of this feature (semicrystalline and highly hydrophilic), the amorphous phase of PVA absorbs water, and thus, this leads to the polymer swelling, and in boiling water, the PVA crystallites can be easily dissolved.[27, 44-47] To limit the swelling and dissolution of PVA, membranes are chemically cross-linked, most commonly using aldehydes and dicarboxylic acids, which under acid catalysis react with PVA to form cross-links.[43, 44, 48] Methods of PVA cross-linking are of great interest since PVA has been industrially used. Today, PVA membranes are still being produced by using chemical cross-linkers and acid catalyst.[30, 49] Physical or thermal cross-linking methods were also proposed to make PVA resistant to water, the key in these methods is the crystallinity.[27, 45, 50-52] By heat treatment or thermal annealing (above glass transition temperature), the PVA chain motion in the amorphous phase (apparent molten state) increases, and because of attraction forces due to the hydrogen bonding, they can form new crystallites and induce the growth of existing crystallites, consequently the crystallinity increases. By freezing-thawing cycles, the crystallinity, and the size of crystallites in PVA can be also controlled, this method has been widely used in the production of hydrogels [27, 53-55] and films for drug-release. [55-57] Thus, new routes of either chemical or physical PVA cross-linking are still of great importance.

In this work, we focus on the design, synthesis and self-assembly of tailor-made PVA-*b*-PS as membrane material. To our knowledge, this is the first report on synthesis of PVA-*b*-PS copolymers with high molecular weight and good film-forming properties. Combining the benchmark hydrophilic block (PVA) with a small hydrophobic domain (PS) within the membrane matrix, we demonstrate that PS nanodomains act as cross-linking points, so chemical cross-linkers and acid catalysts would no longer be needed. We also show that by an additional thermal annealing, the crystallinity of the block copolymer can be enhanced, making the material more resistant to water and solvents. Therefore, the use of this type of

block copolymers in the membrane field would become a breakthrough since the use of regulated chemical compounds (acids and cross-linkers) can be eliminated, and the manufacturing cost of end products could be reduced.

2. Experimental section

2.1. Materials

Styrene (Sty, ≥ 99%, Aldrich) and vinyl acetate (VAc, ≥ 99%, Aldrich) were purified by passing through columns of basic aluminum oxide (Aldrich) and neutral aluminum oxide (Aldrich), respectively (to remove inhibitors prior to use them). 2,2'-Azobis(2-methylpropionitrile) (AIBN, ≥ 98%, Aldrich) was recrystallized from methanol before using it. Anisole (99%, Aldrich), benzyl bromide (98%, Aldrich), copper(II) bromide ($CuBr_2$, 99.99%, Aldrich), tin(II) 2-ethylhexanoate ($Sn(EH)_2$, 92.5-100.0%, Aldrich), tris[2-(dimethylamino)ethyl]amine (Me_6TREN, 97%, Aldrich), sodium azide (NaN_3, 99.5%, Aldrich), *N*,*N*-dimethylformamide (DMF, extra dry, Acros Organics), potassium ethyl xanthogenate (96%, Aldrich), propargyl bromide solution (80 wt.% in toluene, Aldrich), copper(I) bromide (CuBr, 99.99%, Aldrich), tetrahydrofuran (THF, extra dry, Acros Organics), *N*,*N*,*N'*,*N''*,*N''*-pentamethyldiethylenetriamine (PMDETA, 99%, Aldrich), potassium hydroxide (90%, Aldrich), pentane (technical grade, Biosolve), methanol (technical grade, Biosolve), and diethyl ether (technical grade, Biosolve) were used as received. Deuterated chloroform ($CDCl_3$, D 99.8 %) with 0.05 v/v % TMS and deuterated dimethyl sulfoxide (DMSO-d_6) were obtained from Cambridge Isotope Laboratories.
Distilled water and dimethyl sulfoxide (DMSO, ≥ 99.9%, Aldrich) were used for film preparation. Poly(acrylonitrile) (PAN) porous support, Polyvinyl alcohol (PVA, 125kDa), ethanol (technical grade) and commercial cross-linked membrane were supplied by DeltaMem AG.

2.2. Synthesis of poly(vinyl alcohol)-*b*-poly(styrene) copolymers

The amphiphilic block copolymers were synthesized by the combination of reversible-deactivation radical polymerization (RDRP) techniques previously described by Altintas et al. [38] However, for obtaining block copolymers with high molecular weights (> 60kDa) and PVA/PS ratio between 4 and 20 (wt.%/wt.%), the PS and PS-*b*-PVAc synthesis steps were optimized. The copolymer synthesis followed five steps: (1) synthesis of PS homopolymer containing bromine end-group by activators regenerated by electron transfer atom transfer radical polymerization (ARGET-ATRP); (2) bromine end-group substitution by azide

functional group; (3) CTA attachment via CuAAC click reaction; (4) chain extension by reversible addition fragmentation chain transfer (RAFT) polymerization of VAc to obtain PS-*b*-PVAc; (5) hydrolysis of PS-*b*-PVAc to obtain PS-*b*-PVA di-block copolymer. Nonetheless, in this work, the final PS-*b*-PVA copolymer can be indistinctly denoted as PVA-*b*-PS, since the PVA block content is high (>80 wt.%). Details (formulation) of polymerization steps are presented in supporting information.

2.3. Thick dense film and thin film membrane preparation

Casting solutions (3 wt.% copolymer) were prepared by stirring the copolymers (powder) in DMSO overnight (flask immersed in an oil bath at 70 °C). The thick dense films were prepared by casting the homogeneous solution on poly(ether-ether-ketone) (PEEK) plates by using a micrometer-adjustable film applicator (doctor blade 100 mm width, EQ-Se-KTQ-100, MTI Corporation, USA). The gap of doctor blade was adjusted to 200 μm, and the solvent was evaporated at 70 °C for 90 min in a convection oven. Then, the freestanding dense films were peeled off from the PEEK plates and their thicknesses were measured using a micrometer thickness gauge.

Thin film membranes were prepared from aqueous polymer solutions (dispersed micelles). Water was added dropwise to the block copolymer solution obtained above; this process is carried out to obtain a mixture of water/DMSO (80/20 wt.%/wt.%) to trigger the formation of self-assembled micelles. After complete addition of water, DMSO was removed by dialysis through a regenerated cellulose membrane (MWCO 8k Da, RC6, Spectra Por, USA). The resulting aqueous solution was then cast onto the microporous PAN substrate followed by drying in the convection oven (145 °C and 6 min). Both thick dense films and thin film membranes were cut (area=$3.8 \times 10\text{-}5$ m^2) for the characterization.

2.4. Characterization techniques

The chemical structure of the synthesized block copolymers was characterized by proton nuclear magnetic resonance (^{1}H NMR) and by Attenuated total reflection–Fourier transform infrared (ATR–FTIR) spectroscopy. The ^{1}H NMR spectra were recorded using a Bruker Ascend 500 at RT in deuterated chloroform ($CDCl_3$) for PS and PS-*b*-PVAc, while for PVA-*b*-PS, deuterated dimethyl sulfoxide (DMSO-d_6) was used. Chemical shifts (δ) are reported in ppm and quoted in respect to tetramethylsilane (TMS, δ 0.00 ppm). The collected spectra are analyzed using MestReNova (v12.0) (Mestrelab Research S.L). The background-corrected

ATR–FTIR spectra were recorded in a PerkinElmer UATR Two spectrophotometer in the range of 4000–400 cm^{-1}.

The weight and the number average molecular weight values (M_w and M_n) and the polydispersity (PD) were determined by gel permeation chromatography (GPC) using an Agilent system composed of a 1100 series pump, an autosampler, and a refractive index detector (RI) (1260 Infinity II). The GPC system was equipped with a series of linear-S SDV columns (pre-column (5 cm), three analytical columns (30 cm) all with 5 μm particles sizes. All the columns have a diameter of 0.8 cm (PSS polymer, Germany). The RI detector and the columns were kept at 35 °C. $CHCl_3$, stabilized with ethanol is used as the eluent at a flow rate of 1 mL min^{-1}. The system is calibrated with PS standards.

The thermal properties of block copolymers and dense films were characterized by differential scanning calorimetry (DSC) using a DSC 214 Polyma (Netzsch). The copolymer samples were first annealed at 180°C under nitrogen to remove the effect of thermal history. Subsequently, the samples were cooled to 0 °C, and then a heating/cooling cycle with a rate of 10 °C min^{-1} was applied for the scan. For the dense films, one single heating/cooling cycle with a rate of 10 °C min^{-1} was applied. The data analysis was performed using the Netzsch Proteus Software. The glass transition temperature (T_g) values were taken from the onset of transition, and the melting temperature (T_m) values from the maximum of peaks.

Thermogravimetric analysis (TGA) was also performed on copolymer samples, for that, a TGA5500 (TA Instruments) instrument under constant nitrogen flow and coupled to a MKII mass spectrometer was used. After weight stabilization, the temperature was equilibrated at 30 °C before heating at a rate of 10 °C min^{-1} to 550 °C, followed by cooling back down to ambient temperature. The decomposition temperature (T_d) values were taken from the onset of the TGA curve.

The self-assembly of block copolymers in solution was studied by dynamic light scattering (DLS). The hydrodynamic diameter (D_h) of self-assembled nanostructures (15 mg mL^{-1}) was measured with a Zetasizer Nano ZSP (Malvern Instruments). Each measurement was taken at 20 °C after an equilibration time of 300 s with a backscattering angle of 173°.

The self-assembled micelles were microphotographed by a transmission electron microscope (TEM) Philips CM100 at an acceleration voltage of 80 kV. The nanostructured micelles in water (0.1 mg mL^{-1}) were adsorbed on a glow-discharged carbon copper grid and negatively stained with 2% aqueous uranyl acetate.

Static contact angle (CA) measurements were performed to characterize the hydrophilicity of membrane surface. The instrument is a CA goniometer, CAM 100 (LOT quantum design),

based on a CDD camera with 50 mm optics. Droplets of ultrapure water were placed on the sample surface with a micro syringe, and the CA was automatically recorded and analyzed by the instrument software, fitting the experimental curve with the Young–Laplace equation. The drop volume (2 μL) was kept constants for all measurements. The average values and standard deviations were reported based on at least four measurements taken at different location of the surface.

The membrane swelling was characterized on freestanding dense films. The swelling degree (SD) is represented by the water uptake, which was determined gravimetrically in ethanol/water mixture (7 wt.% water). Dried films are immersed into the solvent mixture at RT, then they are left to swell until constant weight. The swollen samples are removed from the mixture, wiped with a filter paper, and weighed. Three parallel measurements were carried out for each sample; the SD values are calculated as follow:

$$SD = \frac{(m_s - m_d)}{m_d} \times 100 \qquad (1)$$

where m_s and m_d are the masses of the swollen and dried films, respectively.

Scanning electron microscope (SEM) was used to measure the thickness of thin film membranes, the images are acquired using a Hitachi S-4800 SEM (Hitachi High-Technologies Corporation, Japan) with a cold field-emission electron source. Electrically conducting surfaces were created by sputtering the sample surface with a gold layer of 5 nm thickness.

The separation performance of dense films and thin film membranes were characterized in a pervaporation bench-top-unit that include two membrane cells (each cell provides an effective area of 3.8×10-5 m^2). An ethanol/water mixture (95.5/4.5, wt.%/wt.%) was used as feed mixture for the pervaporation tests. The operating temperature is 95°C, the feed/retentate pressure 2 bar, and the permeate pressure 10 mbar (kept by a vacuum pump). Permeate samples are collected in cold traps with dry ice/ethanol mixture. For each measurement point, the time, feed/retentate and permeate samples are collected. The water and ethanol concentration of the samples are determined by Karl-Fischer (KF) titration (917 Coulometer, Metrohm) and gas chromatograph (GC) from Agilent, respectively. The separation performance of the membranes can be evaluated based on the permeate concentration (wt.%) and water permeate flux J_i (kg m^{-2} h^{-1}):

$$J_i = \frac{m_i}{A \times t} \qquad (2)$$

where m_i is the amount of water in the permeate (kg), A is the effective membrane area (m^2), and t is the operating time (h) between sample collection.

The separation performance of membranes can be also represented by the permeability (P_i) or permeance (P_i/l) which are the intrinsic properties of the membranes:

$$\frac{P_i}{l} = \frac{J_i}{(x_i \gamma_i p_i^{sat} - y_i p^p)} \qquad (3)$$

where l is the membrane thickness, x_i and y_i are the mole fraction of component i in the feed and permeate, γ_i the activity coefficient of component i in the liquid feed calculated by NRTL theory, p_i^{sat} the saturated vapor pressure of the component i in the feed (calculated using the Antoine equation) and p^p the permeate pressure. The unit of P_i is generally in Barrer (1 Barrer = 1×10^{-10} cm3 (STP) cm cm^{-2} s^{-1} $cmHg^{-1}$).

3. Results and discussion

3.1. Synthesis and structural characterization of block copolymers

The synthesis of PVA-*b*-PS or PS-*b*-PVA copolymers with low M_n and narrow PD is straightforward, as reported by Altintas et al [38] and other authors (Table S1, supporting information). However, when we attempted to synthesize copolymers with high M_n and high content of PVA block, we ran into some limiting factors that hindered the polymerization reaction, *i.e.*, the growth of polymer chain was limited.

To overcome this problem, we first synthesized PS-Br homopolymers according to Altintas et al, the kinetic of polymerization was investigated, and the results showed that high concentration of initiator and catalyst, and low concentration of reducing agent ($Sn(EH)_2$) produce well controlled (PD < 1.10) polymers, but with low M_n. The rate of polymerization was quite linear until the conversion reached 20-30%, and the values of $Ln[M]_0/[M]_t$ increased linearly with time at this stage. However, for longer time of polymerization, both the conversion and the values of $Ln[M]_0/[M]_t$ did not show linearity anymore, they showed a plateau (Fig. S1, supporting information), and thus, polymers with lower M_n than 32kDa were obtained (Table S2, supporting information). As a second step, lower concentration of initiator and catalyst were used to reduce the number of polymer chains and to minimize the β-hydrogen elimination, [58-60] respectively. After several polymerization experiments, the reducing agent ($Sn(EH)_2$) was increased with the aim of regenerating the active catalyst (Cu^I/Ligand), since during the termination process, Cu^{II}/Ligand is formed.[61] Thus, these changes in the formulation allowed obtaining PS-Br homopolymers with higher M_n and high conversion.

The chain extension of PS-CTA by VAc in presence of AIBN was more straightforward, here we only increased the concentration of VAc monomer with respect to PS-CTA macroinitiator,

and both the conversion and the M_n could be controlled (see also Fig. S1 in supporting information).

Figure 1 shows the results of the analysis performed during the PS-*b*-PVA synthesis (e.g., PS_{100}-*b*-PVA_{1639}): the synthesis of PS-Br by ARGET-ATRP (^{1}H NMR and GPC), the bromine substitution by the azide group (GPC), the CTA attachment (GPC), the chain extension by RAFT polymerization of VAc (GPC) and the obtention of PS-*b*-PVA by hydrolysis (^{1}H NMR and ATR-FTIR). The ^{1}H NMR spectra corresponding to PS-Br, PS-N_3, PS-CTA, PS-*b*-PVAc and PS-*b*-PVA are presented in supporting information (Fig S2). Here, we show only the spectra of PS-Br and PS-*b*-PVA (Figure 1a and 1b), the observed peaks are consistent with literature, [38, 40, 41, 62, 63] the characteristic signals corresponding to aromatic protons of the PS block are clearly identified in both spectra, these are associated to the resonance from 7.24 to 6.30 ppm (peaks c, d and e). The signals from 1.62 to 1.33 ppm arise from the aliphatic protons from the block copolymer backbone (peaks a, b, and f) except for the protons adjacent to the hydroxyl groups which appears at 3.84 ppm (peak g). The signals at 4.68, 4.52 and 4.28 ppm are related to the different tacticity of the hydroxyl proton from the PVA block (peak h = isotatic, i = atactic and j = syndiotactic). Last, the peaks marked with an asterisk (*) correspond to the traces of solvents used during synthesis/purification steps, i.e., water and THF in CDCl3 and DMSO-d6, respectively.

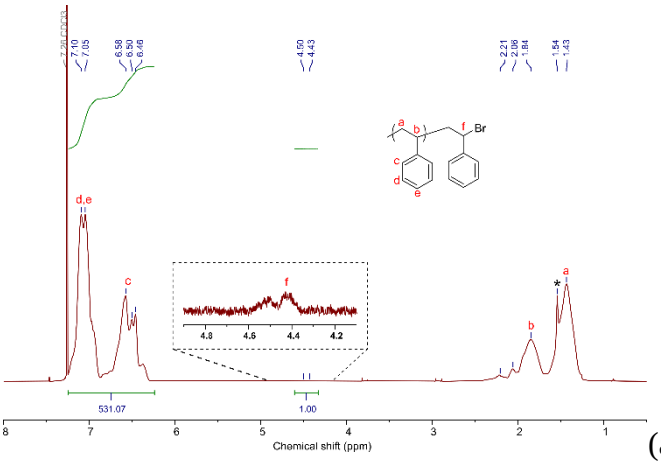

(a)

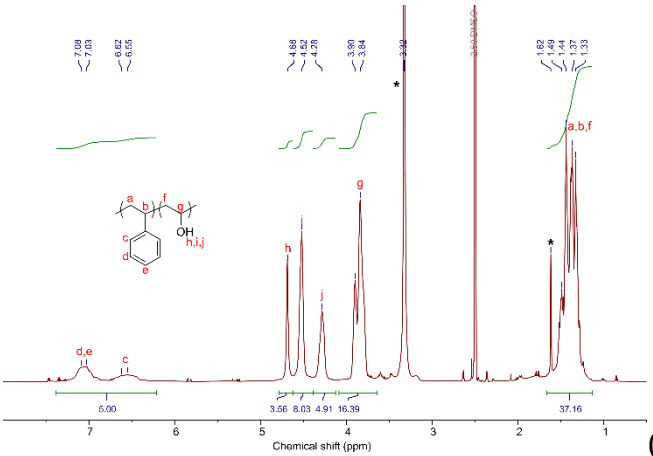

(b)

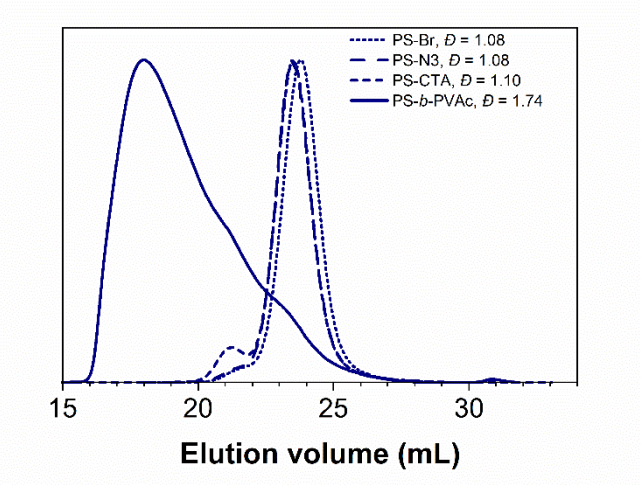

(c)

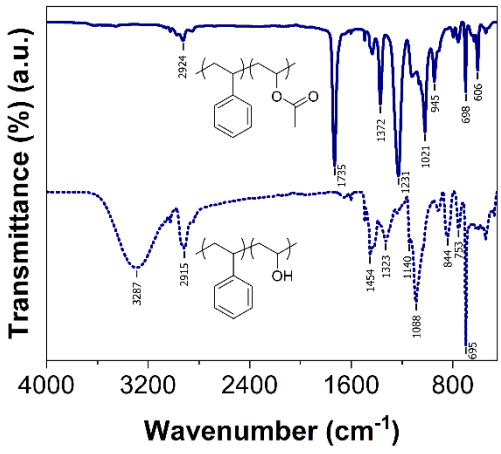

(d)

Figure 1. Chemical structure characterization of synthesized homopolymers and di-block copolymers: (a) ^{1}H NMR spectrum corresponding to PS-Br homopolymer, (b) ^{1}H NMR spectrum of PS-*b*-PVA copolymer, (c) GPC elugrams of PS-Br, PS-N_3, PS-CTA and PS-*b*-PVAc copolymer, and (d) ATR-FTIR spectra of PS-*b*-PVAc and PS-*b*-PVA copolymer.

The change of molecular structure from PS-Br to PS-N_3 to PS-CTA and to PS-*b*-PVAc is nicely monitored by the GPC elugrams (Figure 1c). GPC elugrams at different stages during

the synthesis show that the synthesized PS-Br homopolymer exhibits narrow molecular weight distributions (PD =1.08), this PD value is kept when the bromine group is substituted by the azide group. Later, the PS-CTA shows a slight increase of PD to 1.10. These results confirm a good control of the PS-CTA macroinitiator synthesis. However, in this last step, a small bump appeared at the lower elution volume (21 mL) which would correspond to the formation of small amount of higher molecular weight species. After chain extension of PS-CTA with VAc, the GPC curve corresponding to PS-*b*-PVAc shows a significant shift to lower elution volume, what confirms the increase of molecular weight of polymer, the PD value in this case increased to 1.74. Two small shoulders are also observed, the first one matching to the PS-Br precursor (23.5 mL) and the second one (21 mL) to the PS-CTA. Both small shoulders would correspond to inactive chain ends that did not lead to chain extension, and thus, they contributed to the increase of PD. These small fractions of both PS-Br and PS-CTA can be tolerated in this step, since in the next step (hydrolysis) they should not precipitate. Even though a broader molecular weight distribution is observed, in practice they should be lower when PS-*b*-PVAc is hydrolyzed to PS-*b*-PVA. Compared to other PS-*b*-PVAc reported in the literature (Table S1, supporting information), the PD values that we have obtained are similar or lower.

The full conversion of PVAc block to PVA block is confirmed by ^{1}H NMR (Fig. S2, supporting information) and ATR-FTIR (Figure 1d) analyses. The complete disappearance of C=O stretch at 1735 cm-1 and appearance of the broad O-H signal around 3287 cm-1 confirm that PVAc was completely hydrolyzed.[38, 63, 64] The peaks corresponding to PS (C-H stretching of the benzene ring at 3026 cm-1, carbon ring vibration at 1601 and 1493 cm-1, and the out-of-plane ring vibration at 755, 698 and 540 cm-1)[38, 65] remained unaffected. Besides the confirmation of the successful hydrolysis, a few other characteristic peaks were identified, like the medium band at 2924 cm-1 which is attributed to the stretching of CH groups from the backbone, the increase of the band at 1420 cm-1 that is characteristic for the bending vibrations of the CH2, the medium band at 1323 cm−1 and the strong peak at 1088 cm−1 associated to the OH bending and the C-O stretching of the alcohol group, respectively. The semicrystalline feature of PVA that is represented by the C-O stretching vibration at 1141 cm−1[66, 67] is also observed.

A list of copolymers synthesized for this work are presented in **Table 1**. In addition to the hydrophilic block-copolymers, a block copolymer containing high PS block was synthesized for comparison. The names of block copolymers are referred to PVA content (weight fraction) obtained by ^{1}H NMR spectroscopy. The M_n values are also obtained from the ^{1}H NMR

analysis. As seen, we were able to obtain copolymers with M_n higher than 60kDa and PVA block content higher than 80 wt.%. Because the PS-*b*-PVA copolymers are not soluble in almost all typical solvents used in GPC analyses (Table S3, supporting information), the reported PD corresponds to PS-*b*-PVAc, so we assume that the PD values do not change during the hydrolysis step, or even they decrease due to the presence of inactive PS-Br and PS-CTA that did not precipitate together with PS-*b*-PVA, described above.

Table 1. Composition, conversion, M_n, PD and f_{PVA} of synthesized PS-*b*-PVA copolymers

Sample	Composition [a]	Conversion [%]	M_n [a] [g/mol]	PD [b]	f_{PVA} [a]
PVA-81	PS_{57}-*b*-PVA_{587}	59	32000	1.55	0.81
PVA-31	PS_{298}-*b*-PVA_{318}	5	45000	1.29	0.31
PVA-87	PS_{57}-*b*-PVA_{921}	61	46000	1.49	0.87
PVA-68	PS_{192}-*b*-PVA_{948}	25	61700	1.53	0.68
PVA-79	PS_{139}-*b*-PVA_{1220}	61	68200	1.45	0.79
PVA-87	PS_{100}-*b*-PVA_{1639}	55	82500	1.74	0.87
PVA-92	PS_{56}-*b*-PVA_{1500}	66	71800	2.11	0.92

[a] obtained by ^{1}H NMR; [b] PD corresponds to PS-*b*-PVAc (obtained by GPC)

The copolymers that have high M_n (>60kDa) and high content of PVA block (>80 wt.%) are tailor-made for applications in the membrane field (discussed later). The other copolymers with low M_n and low content of PVA do not show good film-forming property (Fig. S3, supporting information), and are less hydrophilic, and thus, they cannot be used as membrane material. However, they can have potential applications in others field.

3.2. Thermal characterization of block copolymers

DSC measurements and TGA were performed to determine the T_g, T_m, crystallinity, and T_d of homopolymers (PS and PVA) and block copolymers (**Figure 2**), respectively. The DSC thermograms are displayed in Figure 2a, these thermograms confirm that the copolymers are constituted by two blocks that tend to microphase separation (presence of two glass transitions). The first transition observed between 74 and 81 °C corresponds to the glass transition of PVA,[68] while those between 103 and 105 °C to the glass transition of PS.[69] The T_g of the short block either PS or PVA in the block copolymers (PVA-92 and PVA-31) cannot

be distinguished, this can be because when a polymer segment of the block copolymer decreases in length, its T_g can be suppressed relative to the other segment.[70] At 180 °C, an endothermic peak corresponding to the melting transition of the PVA crystalline domains appears,[50, 68, 71] from this endothermic peak we obtained the T_m (>220°C) and the crystallinity of PVA block. The fraction of crystallinity is calculated from the ratio between the enthalpy of fusion from the endothermic melting peak (ΔH_f) of sample and the enthalpy of fusion of the totally crystalline polymer PVA (ΔH_f^0) by using ΔH_f^0 = 138.6 J g^{-1}.[50]

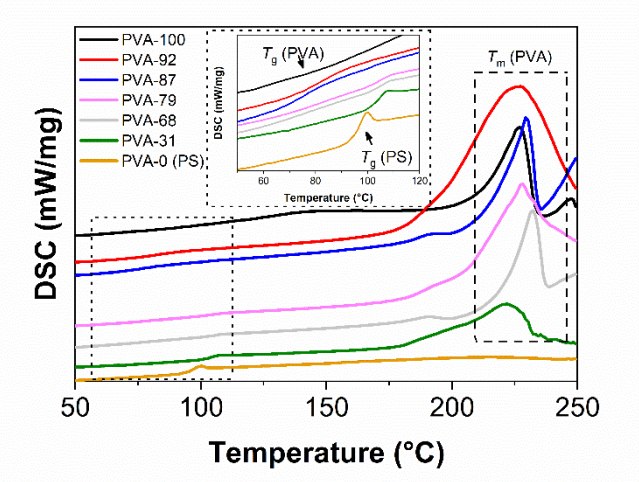

(a)

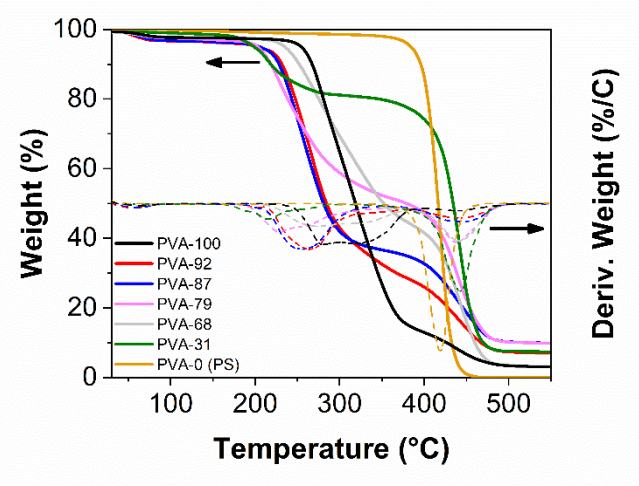

(b)

Figure 2. DSC (a) and TGA (b) thermograms for PVA and PS homopolymers and for PS-*b*-PVA copolymers

The TGA shows three distinct degradation regions (Figure 2b), the first weight loss (ca. 100 °C) is attributed to the evaporation of water, which is absorbed by the hydrophilic samples (except the PS homopolymer). From ca. 200 °C to 240 °C, the decomposition of PVA starts, and the lowest value corresponds to the copolymer with low M_n and low content of PVA, while the other copolymers exhibit higher values of T_d, which are expected because

the M_n and PVA content in the copolymers increase. The second weight loss is observed in the range of 400-450 °C, this T_d corresponds to PS. All thermal properties corresponding to the copolymers of interest and homopolymers are summarized in **Table 2**.

Table 2. Thermal properties of PS, PVA and PS-*b*-PVA copolymers with high M_n

Sample	T_g^{PVA} [°C]	T_g^{PS} [°C]	T_m^{PVA} [°C]	Crystallinity [%]	T_d^{PVA} [°C]	T_d^{PS} [°C]
PVA-0 (PS)	n.a.	95.2±0.3	n.a.	n.a.	n.a.	401.0
PVA-31	-	103.4±0.1	223.1±1.1	27.4±1.6	192.0	418.0
PVA-68	72.1±0.1	105.4±0.4	231.8±0.4	32.4±1.7	237.0	419.0
PVA-79	74.8±1.5	104.4±0.6	226.4±1.4	35.6±2.8	207.0	416.0
PVA-87	75.2±0.9	103.2±1.8	229.1±0.6	39.6±1.2	225.0	405.0
PVA-92	77.4±1.3	-	231.5±0.2	52.6±0.6	231.0	411.0
PVA-100	76.4±0.2	n.a.	229.0±1.4	55.2±1.7	250.0	n.a.

The full conversion of PVAc to PVA by hydrolysis was also confirmed by DSC (Fig. S4, supporting information). For the PS-*b*-PVAc, the thermogram shows that the block copolymers are amorphous, i.e., only glass transitions of each block are observed (e.g., T_g^{PVAc} = 39.7 °C and T_g^{PS} = 101.8 °C). However, after the hydrolysis of PVAc block to PVA, the T_g corresponding to PVAc disappears completely, and the endothermic peak corresponding to the PVA melting transition appears.

According to the DCS analysis, the copolymers are composed by two separated microphases, one that corresponds to PS amorphous phase, and the other one where PVA amorphous and crystalline phase coexist. The interesting of these copolymers is that PS is completely amorphous, glassy, and acts as barrier, while PVA is semicrystalline, and its amorphous phase can swell in presence of water. The swollen state of this phase allows permeating water and other molecules depending on molecular size and affinity. Thus, these features give the possibility of tunning the final transport property of material.

3.3. Thick dense film preparation and characterization

As this block copolymers are not soluble in common solvents (Table S3, supporting information), the Hansen Solubility Parameters (HSP) of each block were plotted together with those of common solvents (**Figure 3**). This 3D plot helps to identify possible

formulations (mixtures of solvents) which may allow obtaining a homogeneous solution. The dashed line (grey) between the PS and PVA core represents the calculated parameters according to the hydrophilic block content, e.g., for a balanced ratio (50/50 wt.%/wt.%), DMAc should be an ideal candidate because the HSP values are in the middle of the line. The choice of this solvent is in good agreement with the literature, since PS-*b*-PVA block copolymers with low M_n and low PVA content were dissolved in DMAc.[38] In our case, the dissolution of PVA-*b*-PS with high M_n and high PVA content turned out to be impossible. Other solvents and mixtures thereof did not provide satisfying results, and after several attempts, the only solvent that dissolved to the block copolymers was hot DMSO, except to PVA-31 block copolymer that has high content of PS block.

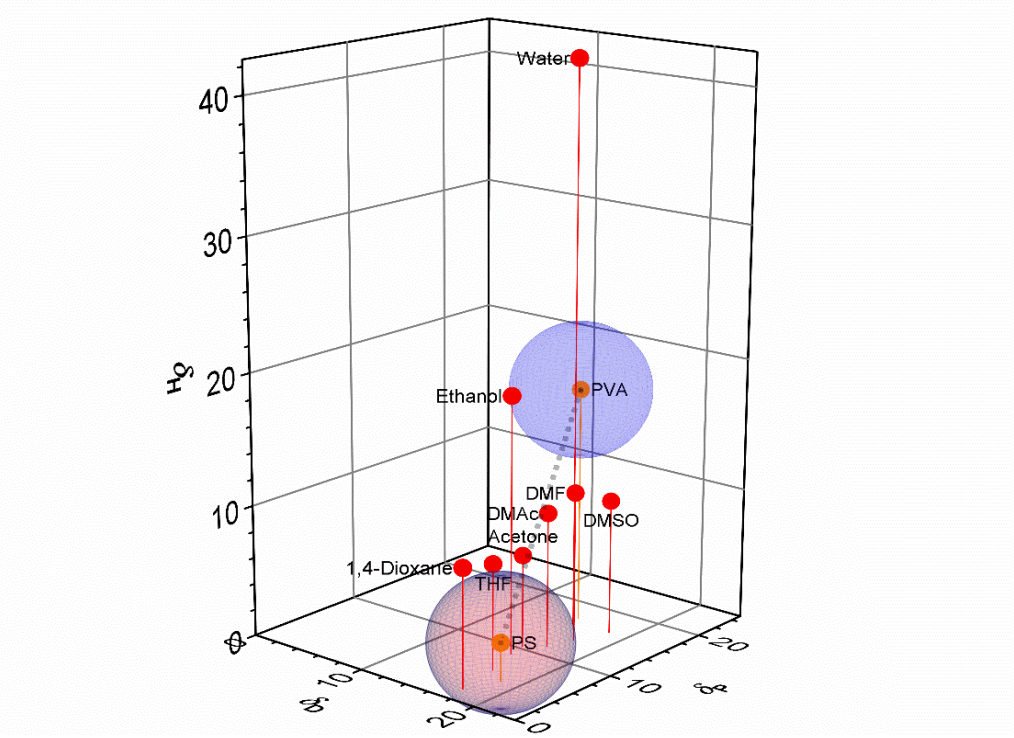

Figure 3. Representation of the Hansen Solubility Parameters in 3D space for PVA, PS, PVA-*b*-PS and typical solvents used for membrane preparation

Self-standing dense films with thicknesses ranging between 15-20 μm were prepared by casting from solutions of block copolymer in DMSO. For comparison purposes, commercial PVA and PS homopolymers (referred as PVA-100 and PVA-0) films were also prepared. Contact angle measurements performed on the self-standing films (**Figure 4a**) shows that the block copolymer samples are less hydrophilic than the sample prepared from PVA homopolymer, which is correlated with the PVA content. The PVA film shows the lowest CA value (57°), while the PS film the highest one (95°). Interestingly, the CA values of the block

copolymer films increase in a very cute way as the PS content increases. Compared to the chemically cross-linked PVA (55°),[72] the block copolymer films exhibit high values of CA. Although the CA values of copolymer films slightly increase (from 74.9° to 83.5°) as the PS content increases, the degree of swelling of samples (**Figure 4b**) in ethanol/water mixture is almost the same (ca. 20%), which means that the content of PS block (<32 wt.%) in these copolymers did not affect the swelling of block copolymer films. These results could be attributed to three factors: 1) a balance between PVA content in the copolymer and PVA amorphous fraction, i.e., high PVA content balances the low amorphous fraction of PVA (see Table 1 and 2), 2) the slight variation of M_n (Table 1), and 3) the water content in the mixture (7 wt.% water in ethanol) used for the swelling tests. The fact of using ethanol/water mixture instead of water for the swelling test is to obtain realistic results that represent the medium where the membranes will be used, since the swelling tests are important for the membrane material, because the separation performance and stability of polymeric membranes depend strongly on swelling degree of material. Last, the PS film did not swell at all, and the chemically cross-linked PVA swelled up only 5%.

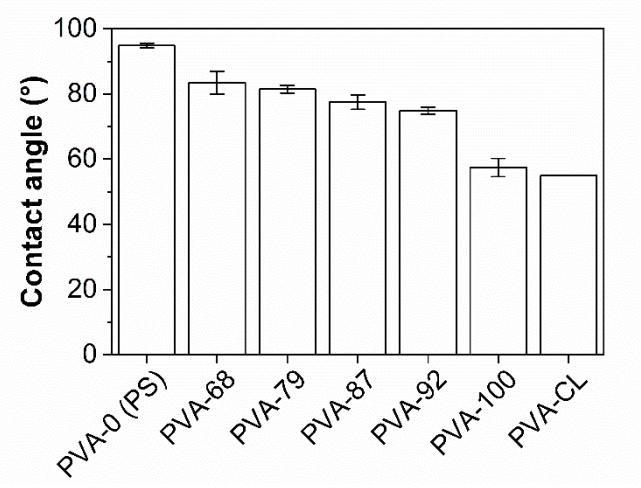

(a)

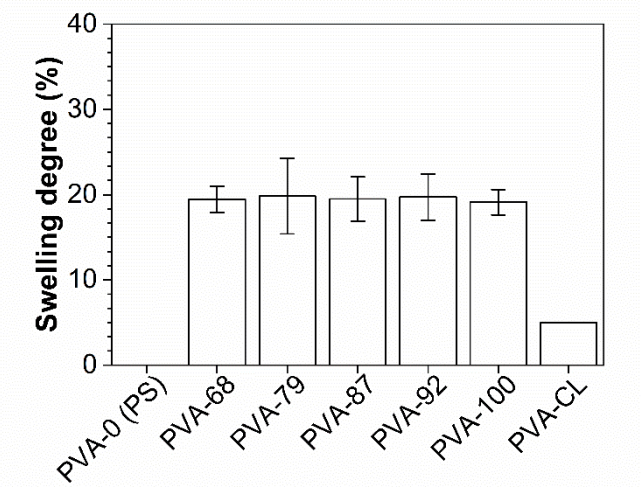

(b)

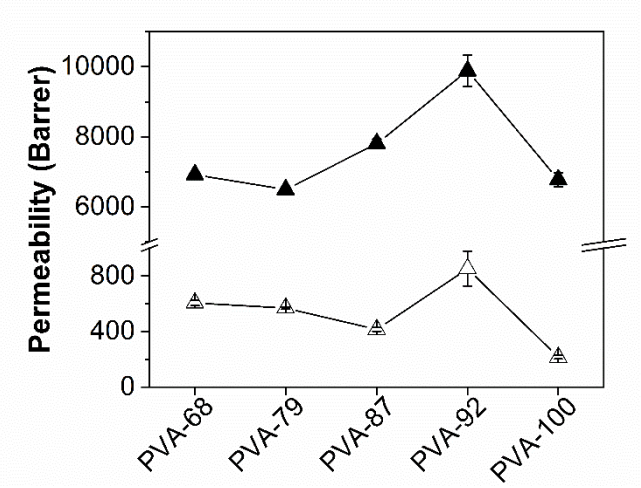

(c)

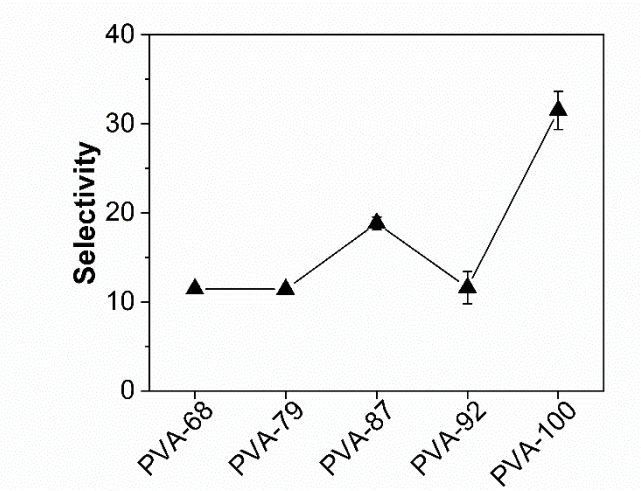

(d)

Figure 4. Properties of self-standing dense films: (a) Contact angle, (b) swelling degree, (c) water (filled experimental points) and ethanol (unfilled experimental points) permeability, and (d) water/ethanol selectivity

Figure 4c shows the water and ethanol permeability through the dense films. Those were obtained by carrying out pervaporation tests (feed: ethanol/water mixture with 4.5 wt.% water, operating temperature: 95°C, and permeate pressure: 10mbar). The water permeability values for the copolymer membranes with less than 80% of PVA block are lower than those with 87% and 92%. This result is attributed to the PVA hydrophilicity (Figure 4a), i.e., the higher the hydrophilicity of membrane, the higher the water permeability. [43, 73] However, the PVA homopolymer sample showed even lower water permeability, which was not expected and is contrary to the previous statement. Therefore here, the PS domain played an important role. In films from PVA homopolymer, the polymeric chains of PVA crystallized significantly, which resulted in higher crystallinity and less PVA permeable amorphous phase, hence it led to lower water permeability. In films from PVA-*b*-PS copolymers, the presence of

PS nanodomains hindered the PVA crystallization and thus, it led to less crystallinity (Table S4, supporting information). Therefore, a controlled quantity of PS domain allowed to obtain potential membrane materials like PVA-87 and PVA-92.

As seen, the water permeability increases slowly as the PS content decreases within PVA matrix until reaching a maximum (PVA-92), these results agree with the hydrophilicity nature of the copolymers. This means the affinity of water molecules are favored as the PVA content in the block copolymer increases.

On the other hand, the water/ethanol selectivity values for the block copolymer films are lower than the sample prepared from PVA homopolymer. The PVA film shows the highest value of selectivity (ca. 30), because the crystallinity is high and the homopolymer is the most hydrophilic, where the water affinity is high. This behavior fits well with the tradeoff of polymeric membranes, the higher the selectivity, the lower the permeability (see Figure 4c and 4d).

In block copolymer films, the water/ethanol selectivity shows a maximum that could be between 80 and 95 wt.% of PVA content. As the water permeability also show a maximum around 92 wt.% of PVA, we believe this to be due to the nanostructure of block copolymer. At the beginning of this work, we targeted to synthesize tailor-made block copolymers with PVA content higher than 80 wt.% and high M_n, and we hypothesized that small quantity of PS nanodomains within the PVA matrix will act as cross-linking points without affecting much the separation performance of PVA membranes. Surprisingly, here we confirm our hypothesis. According to Bates and Frederickson, [9, 74] and Groot and Madden, [75] the self-assembly of di-block copolymers and its nanostructure domains can be predicted knowing χN and f (where χ is the Flory-Huggins parameter, N is the polymer length, and f the ratio of block size). So, the copolymer PVA-92 falls within the disorder region and the resulting nanostructure may be disorder cubic arrays, and the PVA-87 enters in the cubic symmetry phase with ordered nanodomains as body centered cubic structure. Thus, the characteristic of these nanostructures supports the water permeability results, since a cylindrical and/or lamellar nanostructure would lead to lower water permeability due to the PS continuous nanodomains that would act as impermeable phases.

The nanostructure in melt, the properties, and the self-assembly of these block copolymers (for the entire range of composition) will be investigated and discussed in a separated work. Here, we only focus on block copolymers with >80 wt.% of PVA block and high M_n.

3.4. Self-assembly of block copolymers in solution

Obtaining ordered nanostructures with block copolymers is complicated because different factors such as substrate, polymer solution concentration, thickness of the thin film, method of preparation, ambient conditions, method of post treatment among others affect the self-assembly. Thus, the control of nanostructure formation by different methods is considered crucial for obtaining large areas (m^2) of thin films or membranes. [13, 19, 76-78]

To induce and control the self-assembly of block copolymers, we used the method of "solvent switch" by dialysis (**Figure 5**), this method is very versatile because allows controlling the solvent exchange rate and the final solute concentration. First, the PVA-*b*-PS copolymer is dissolved in DMSO (3 wt.%), as described in experimental part. Second, water is added dropwise to the solution; while water is being added, the block copolymer chains start to self-assemble to form micelles with PS block as core, surrounded by PVA as shell, this happens because the medium is aqueous and the PVA block is hydrophilic. Third, when DMSO is completely removed by dialysis, the self-assembled micelles coexist in water and are stable (Fig. S5, supporting information). Last, the self-assembled micelles dispersed in water can be cast onto a substrate to obtain nanostructured thin films.

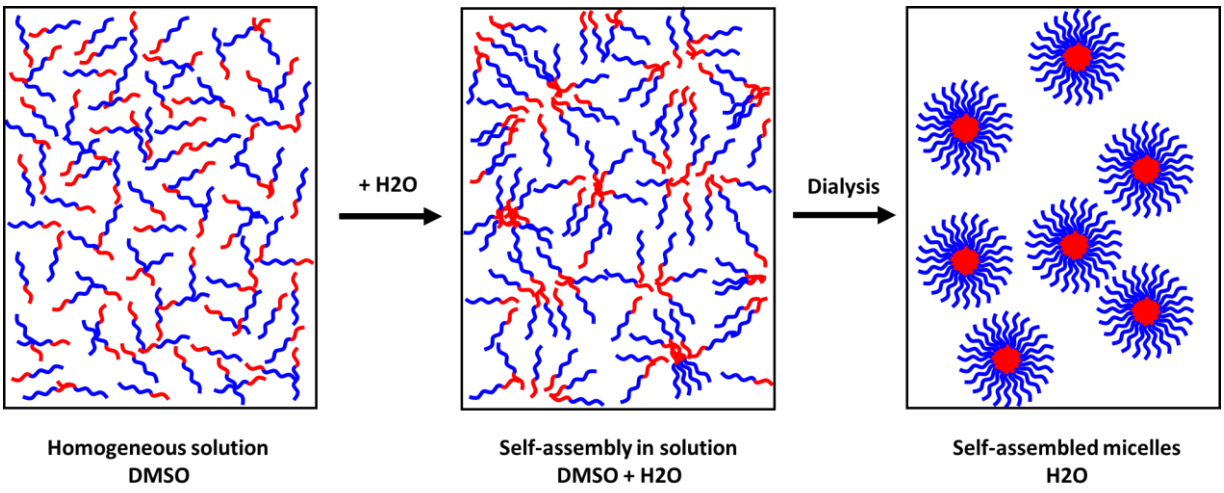

Figure 5. Self-assembly of PVA-*b*-PS copolymer in solution by "solvent switch" method

The prepared PVA-*b*-PS micelle solutions were characterized by DLS and TEM (**Figure 6**). The DLS results show the presence of a trimodal distribution, the first peaks correspond to the single micelles, whereas the second and the third one would correspond to aggregates that resulted due to the aggregation of single micelles because of strong hydrogen bonding between PVA shells. The highest intensity peak corresponds to single micelles with $D_h \approx$ 70nm, 90nm and 100nm, for PVA-92, PVA-87, and PVA-79 copolymers, respectively. Compared to literature, [35, 41, 79, 80] the measured sizes are in good agreement, considering the

high molecular weight obtained in this work. The aggregates have larger diameters, 400nm, 700nm and 5µm, respectively. Because the samples were not filtered, formation of aggregates were expected, since typical protocols for DLS analysis include sample filtration. In our case, the samples were not filtered because the solution is used for the thin film preparation as it is obtained.

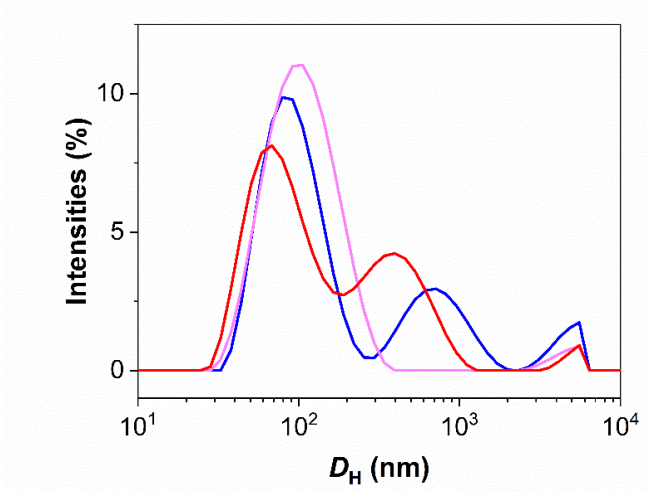

(a)

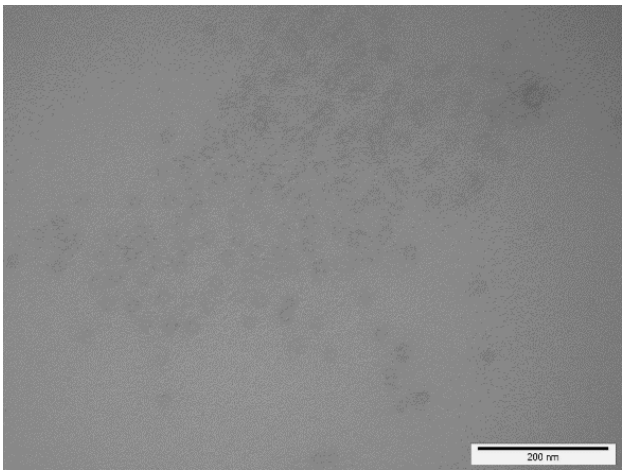

(b)

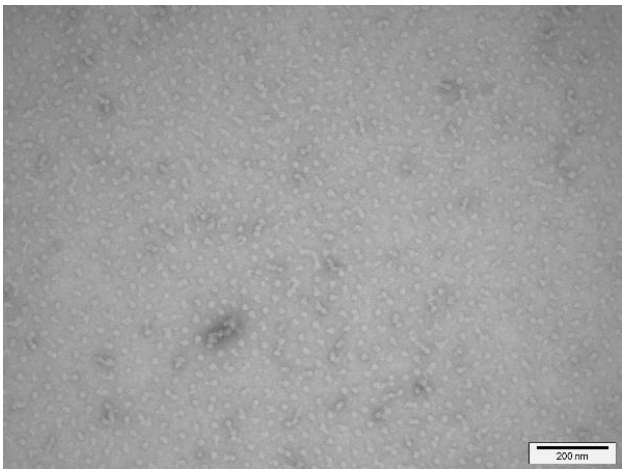

(c)

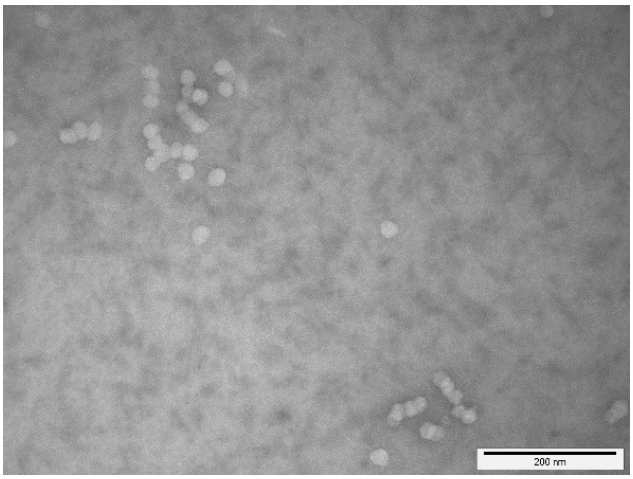

(d)

Figure 6. DLS results corresponding to PVA-92 (red line), PVA-87 (blue line) and PVA-79 (pink line) in aqueous solution (a), TEM micrographs of PVA-92 (b), PVA-87 (c), and PVA-79 (d)

TEM images confirmed the self-assembly (Figure 6b, 6c and 6d) of block copolymers in solution. The images reveal the presence of a plethora of micellar nanostructures, the presence of worm-like structures also confirm that the micelles tend to aggregate, as observed in DLS analysis. Although many micelles are partially aggregated, it is possible to measure the diameters of the dried single micelle nanostructure, which are 19 ± 2 nm. Compared to DLS analysis, the D_h values obtained by TEM are lower, however they are expected due to the differences in the methods used and sample nature. In DLS, the single micelles are highly swollen and due to the PVA content and concentration of solutions (15 mg mL^{-1}), the single micelles are big and tend to aggregate in a greater extent, while for the TEM analysis the solution is diluted (0.1 mg mL^{-1}), the nanostructures are frozen trapped and dried, and thus, the single micelles and aggregates shrink.

3.5. Thin films from self-assembled micelles

Although self-standing thin films are possible to obtain as small samples (Fig. S6, supporting information), for practical purposes, thin films onto PAN porous substrate were prepared from the self-assembled micelles in solution. Because the micelles are dispersed in water and does not contain any chemical cross-linkers or acid catalysts, we think our process is very clean and innovative green process.

Our approach of using these tailor-made copolymers is to leave out the chemical cross-linkers during the PVA membrane preparation (state-of-the-art of PVA membranes includes the use of chemical cross-linkers).

The thin film membranes prepared from these block copolymers would show interesting separation performance due to the nanostructure within the membrane matrix. The micelles in solution after the casting aggregate as the water evaporates, and when they are dried, the PVA blocks make up the matrix of membrane and the dispersed PS nanodomains act as cross-linking points. Thus, this membrane would no longer need chemical cross-linkers.

We selected the PVA-87 sample to prepare thin film membranes, according to the copolymer composition and micelle formation in the aqueous solution, the resulting membrane would be composed of a PVA matrix with PS nanodomains uniformly distributed as body centered cubic structure. For comparison, thin film from PVA homopolymer was also prepared under same conditions.

Figure 7 shows the separation performance of thin films (permeance and selectivity) as a function of temperature of thermal annealing or heat treatment (HT). As expected, the water permeance in block copolymer thin films is higher (~100%) than that in PVA homopolymer (Figure 7a), and a thermal annealing (145 °C and 160 °C) of the thin films led to lower water permeances, but still higher than PVA homopolymer film. Thermal annealing of block copolymers is applied to induce molecular organization and to improve the microphase separation. [81, 82] In addition, thermal annealing induces crystallization of PVA chains, [45, 50] and thus, the permeability or permeance decreases. In samples annealed or heat treated at 160°C, the water permeance decreased more than 50% compared to the no-heat treated sample. In the case of ethanol permeance, the decrease is more pronounced, i.e., after the heat treatment at 145 or 160°C, the ethanol permeance in block copolymer films decreased by a factor of 15 and 45, respectively. These results confirm that within the membrane matrix, the microphase separation between blocks and the PVA crystallinity are enhanced because of thermal annealing (Fig. S7, supporting information). In PVA homopolymer film, the permeance decrease is attributed only to the increase of crystallinity.

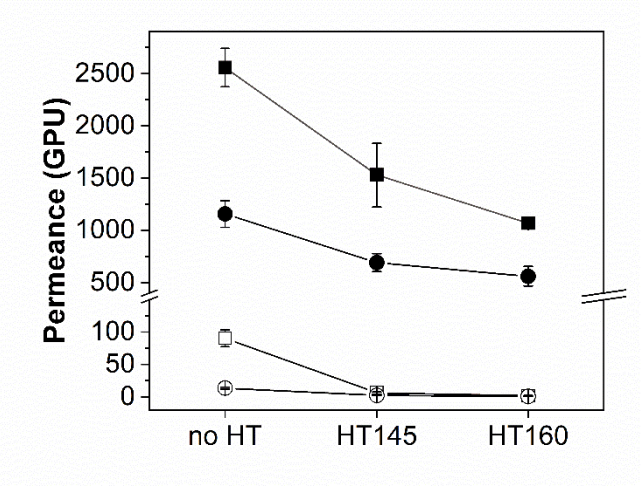

(a)

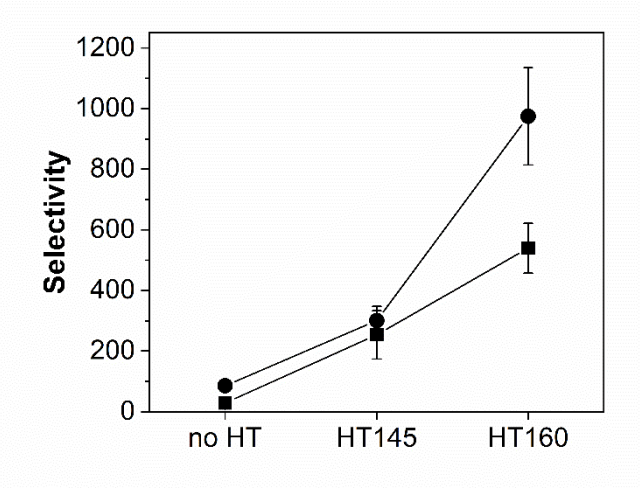

(b)

Figure 7. Separation performance of thin film membranes for PVA-87 block copolymer (square experimental points) and PVA homopolymer (circle experimental points); (a) water (filled points) and ethanol (unfilled points) permeance, and (b) water/ethanol selectivity

Due to the enhanced microphase separation and increased PVA crystallinity, the water/ethanol selectivity in the block copolymer thin films increased by a factor of nine after a heat treatment at 145°C. A subsequent heat treatment at 160 °C, the selectivity enhancement is almost by a factor of twenty. These changes in the membrane performance are impressive and are explained by the nature of block-copolymer, i.e., the fraction of free volume decreased within the PVA amorphous region due to the presence of cross-linking points because of both, the PS nanodomains and the PVA crystallites (enhanced by thermal annealing). Therefore, the ethanol transport is hindered in greater extent than the water transport, what results in higher water/ethanol selectivity values.

The thickness of thin films is ca. 1000 nm. SEM micrographs of thin film membranes are presented in supporting information (Fig. S8).

4. Conclusion

Tailor-made PVA-*b*-PS copolymers with high molecular weight (>70kDa), and high content of PVA (>80 wt.%) were successfully synthesized by ARGET-ATRP and RAFT techniques. To reach our target, we optimized the synthesis of block copolymer by decreasing the concentration of initiator and catalyst during the polymerization, and by increasing the reducing agent (Sn(EH)2) and VAc monomer with respect to PS-CTA macroinitiator. These changes led to reduce the birth of new polymer chains, to minimize the β-hydrogen elimination, to regenerate the active catalyst, and to extend the length of final polymeric chain, respectively.

The chemical structure of synthesized block copolymers and their thermal properties were confirmed by different analysis techniques. The most important features of these copolymers are the good film-forming property and their solubility in solvents. They are not soluble in any solvent, except hot DMSO. Thus, these copolymers can be considered as solvent resistant materials. Nevertheless, by switching the solvent by dialysis, self-assembled micelles in water can be obtained.

Self-standing films were prepared by using DMSO and characterized in terms of permeability and selectivity as membrane material for pervaporation applications. Although the block copolymer films are less hydrophilic than PVA homopolymer, the water permeability is high when ca. 10 wt.% of PS is present in the block copolymer chain. Those results were attributed to the nanostructure of block copolymer because of microphase separation, i.e., the membranes with disordered nanodomains (disorder cubic arrays) and ordered nanodomains as body centered cubic structure exhibit higher water permeability than that in PVA homopolymer. At the same time, we confirmed that PS nanodomains would be acting as cross-linking points.

Because the block copolymers are not soluble in any solvent, we investigated the switch of solvent from DMSO to water by dialysis. By using this method, we demonstrated the control of self-assembly of these block copolymers in solution (aqueous media), i.e., by adding water to DMSO solution in a controlled way, the block copolymers form micelle nanostructures, and then, when DMSO is completely removed, the micelles (70-100nm) coexist and are stable in the aqueous solution. The formation of micelles was confirmed by DLS and TEM.

The self-assembled micelle solution later can be cast onto a porous substrate to form thin film membranes. The thin film membranes obtained in this form confirmed the higher water permeance than that in PVA homopolymer. By a subsequent thermal annealing of thin films, the water permeance decreased (more than 50%), but it was still higher than that in PVA homopolymer. However, the selectivity of membrane was extremely enhanced (up to a factor of twenty). These results were attributed to the improved microphase separation of block copolymers and to the crystallinity increase of PVA block due to the thermal annealing. Due to the PS domains present in the PVA matrix, we also demonstrated that chemical cross-linkers are not needed anymore to make PVA membranes.
Although these block copolymers are still in laboratory stage (complex synthesis, therefore expensive), we believe that in a near future, simpler synthetic methods will be developed. Thus, this kind of tailor-made block copolymers might have a great impact in the membrane field.

Supporting Information

Supporting Information is available from the Wiley Online Library or from the author.

Acknowledgements

This research work was supported by the Swiss Innovation Agency (Innosuisse, project number: 27683.1 PFNM-NM), former Commission for Technology and Innovation (CTI). The authors gratefully acknowledge the financial support from the Swiss National Science Foundation (SNF), Swiss Nanoscience Institute and University of Basel, as well as to the team of Nano Imaging Lab of the Swiss Nanoscience Institute, University of Basel, for assistance with the SEM images. The authors also thank to David Gladman for reading and editing the English. The pervaporation tests were supported by DeltaMem AG, Switzerland.

Received: ((will be filled in by the editorial staff))
Revised: ((will be filled in by the editorial staff))
Published online: ((will be filled in by the editorial staff))

References

[1] https://www.un.org/sustainabledevelopment/energy/, accessed: October, 2022.

[2] P. Mansky, C. K. Harrison, P. M. Chaikin, R. A. Register, N. Yao, Applied Physics Letters 1996, 68, 2586.

[3] A. Urbas, R. Sharp, Y. Fink, E. L. Thomas, M. Xenidou, L. J. Fetters, Advanced Materials 2000, 12, 812.

[4] S. B. Darling, Energy & Environmental Science 2009, 2, 1266.

[5] J. Pyun, T. Kowalewski, K. Matyjaszewski, Macromolecular Rapid Communications 2003, 24, 1043.

[6] A. Car, C. Stropnik, W. Yave, K.-V. Peinemann, Advanced Functional Materials 2008, 18, 2815.

[7] B. Jeong, Y. H. Bae, D. S. Lee, S. W. Kim, Nature 1997, 388, 860.

[8] M. A. R. Meier, S. N. H. Aerts, B. B. P. Staal, M. Rasa, U. S. Schubert, Macromolecular Rapid Communications 2005, 26, 1918.

[9] F. S. Bates, Science 1991, 251, 898.

[10] T. Thurn-Albrecht, J. Schotter, G. A. Kästle, N. Emley, T. Shibauchi, L. Krusin-Elbaum, K. Guarini, C. T. Black, M. T. Tuominen, T. P. Russell, Science 2000, 290, 2126.

[11] I. W. Hamley, "Introduction to Block Copolymers", in Developments in Block Copolymer Science and Technology, 2004, p. 1.

[12] U. Jeong, D. Y. Ryu, D. H. Kho, J. K. Kim, J. T. Goldbach, D. H. Kim, T. P. Russell, Advanced Materials 2004, 16, 533.

[13] K.-V. Peinemann, V. Abetz, P. F. W. Simon, Nature Materials 2007, 6, 992.

[14] J. Ruokolainen, R. Mäkinen, M. Torkkeli, T. Mäkelä, R. Serimaa, G. t. Brinke, O. Ikkala, Science 1998, 280, 557.

[15] M.-L. Wu, D. Wang, L.-J. Wan, Nature Communications 2016, 7, 10752.

[16] M. Gopinadhan, P. Deshmukh, Y. Choo, P. W. Majewski, O. Bakajin, M. Elimelech, R. M. Kasi, C. O. Osuji, Advanced Materials 2014, 26, 5148.

[17] H. Yu, X. Qiu, S. P. Nunes, K.-V. Peinemann, Angewandte Chemie International Edition 2014, 53, 10072.

[18] B. Sutisna, G. Polymeropoulos, V. Musteata, K.-V. Peinemann, A. Avgeropoulos, D.-M. Smilgies, N. Hadjichristidis, S. P. Nunes, Mol Syst Des Eng 2016, 1, 278.

[19] M. J. Fasolka, A. M. Mayes, Annual Review of Materials Research 2001, 31, 323.

[20] S. Y. Yang, I. Ryu, H. Y. Kim, J. K. Kim, S. K. Jang, T. P. Russell, Advanced Materials 2006, 18, 709.

[21] W. Yave, H. Huth, A. Car, C. Schick, Energy & Environmental Science 2011, 4, 4656.
[22] N. Yan, Z. Wang, Y. Wang, Journal of Membrane Science 2018, 568, 40.
[23] Y.-W. Chiang, J.-J. Chang, C.-Y. Chou, C.-S. Wu, E.-L. Lin, E. L. Thomas, Advanced Optical Materials 2015, 3, 1517.
[24] A. Jung, V. Filiz, S. Rangou, K. Buhr, P. Merten, J. Hahn, J. Clodt, C. Abetz, V. Abetz, Macromolecular Rapid Communications 2013, 34, 610.
[25] E. Chiellini, A. Corti, S. D'Antone, R. Solaro, Progress in Polymer Science 2003, 28, 963.
[26] M. N. Tousignant, N. A. Rice, A. Peltekoff, C. Sundaresan, C. Miao, W. Y. Hamad, B. H. Lessard, Langmuir 2020, 36, 3550.
[27] C. M. Hassan, N. A. Peppas, "Structure and Applications of Poly(vinyl alcohol) Hydrogels Produced by Conventional Crosslinking or by Freezing/Thawing Methods", in Biopolymers · PVA Hydrogels, Anionic Polymerisation Nanocomposites, Springer Berlin Heidelberg, Berlin, Heidelberg, 2000, p. 37.
[28] R. Gref, Y. Minamitake, M. T. Peracchia, V. Trubetskoy, V. Torchilin, R. Langer, Science 1994, 263, 1600.
[29] https://www.kuraray-poval.com/applications, accessed: October, 2022.
[30] https://www.deltamem.ch/, accessed: October, 2022.
[31] https://www.ineos-styrolution.com/index.html, accessed: October, 2022.
[32] M. Imoto, T. Otsu, J. Yonezawa, Die Makromolekulare Chemie 1960, 36, 93.
[33] P. Bataille, N. Charifi-Sandjani, Journal of Polymer Science: Polymer Chemistry Edition 1978, 16, 2527.
[34] Z. Lu, X. Huang, J. Huang, Journal of Polymer Science Part A: Polymer Chemistry 1998, 36, 109.
[35] H. J. Jeon, J. H. Youk, Macromolecules 2010, 43, 2184.
[36] J. Muller, F. Marchandeau, B. Prelot, J. Zajac, J.-J. Robin, S. Monge, Polymer Chemistry 2015, 6, 3063.
[37] D. Quémener, T. P. Davis, C. Barner-Kowollik, M. H. Stenzel, Chemical Communications 2006, 5051.
[38] O. Altintas, J. C. Speros, F. S. Bates, M. A. Hillmyer, Polymer Chemistry 2018, 9, 4243.
[39] F. Rajput, A. Colantuoni, S. Bayahya, R. Dhane, P. Servio, M. Maric, Journal of Polymer Science Part A: Polymer Chemistry 2018, 56, 2445.

[40] M. Wang, X. Jiang, Y. Luo, L. Zhang, Z. Cheng, X. Zhu, Polymer Chemistry 2017, 8, 5918.
[41] A. K. Mishra, C. Choi, S. Maiti, Y. Seo, K. S. Lee, E. Kim, J. K. Kim, Polymer 2018, 139, 68.
[42] Y.-J. Chen, B.-J. Wu, F.-S. Wang, M.-H. Chi, J.-T. Chen, C.-H. Peng, Macromolecules 2015, 48, 6832.
[43] N. M. Farhan, S. S. Ibrahim, L. Leva, W. Yave, Q. F. Alsalhy, Chemical Engineering and Processing - Process Intensification 2022, 174, 108863.
[44] B. Bolto, T. Tran, M. Hoang, Z. Xie, Progress in Polymer Science 2009, 34, 969.
[45] T. Hiroyuki, S. Syûzô, N. Isamu, Bulletin of the Chemical Society of Japan 1955, 28, 559.
[46] M. Krumova, D. López, R. Benavente, C. Mijangos, J. M. Pereña, Polymer 2000, 41, 9265.
[47] S. Jeck, P. Scharfer, W. Schabel, M. Kind, Journal of Membrane Science 2012, 389, 162.
[48] https://ntrs.nasa.gov/citations/19790012957, accessed: October, 2022.
[49] M. Frania, A. Huebner, E. Maus (DeltaMem AG), US 9,873,091 B2, 2018.
[50] N. A. Peppas, E. W. Merrill, Journal of Applied Polymer Science 1976, 20, 1457.
[51] S. H. Hyon, H. D. Chu, R. Kitamaru, Bulletin of the Institute for Chemical Research, Kyoto University 1975, 53, 367.
[52] Y. Ueda, T. Tanaka, A. Iizuka, Y. Sakai, T. Kojima, S. Satokawa, A. Yamasaki, Industrial & Engineering Chemistry Research 2011, 50, 1023.
[53] S. R. Stauffer, N. A. Peppast, Polymer 1992, 33, 3932.
[54] N. A. Peppas, S. R. Stauffer, Journal of Controlled Release 1991, 16, 305.
[55] N. A. Peppas, J. E. Scott, Journal of Controlled Release 1992, 18, 95.
[56] A. Takamura, F. Ishii, H. Hidaka, Journal of Controlled Release 1992, 20, 21.
[57] J. C. Flores-Arriaga, D. Chavarría-Bolaños, A. d. J. Pozos-Guillén, V. A. Escobar-Barrios, B. I. Cerda-Cristerna, Journal of Materials Science: Materials in Medicine 2021, 32, 56.
[58] K. Matyjaszewski, W. Jakubowski, K. Min, W. Tang, J. Huang, W. A. Braunecker, N. V. Tsarevsky, Proceedings of the National Academy of Sciences 2006, 103, 15309.
[59] W. Jakubowski, B. Kirci-Denizli, R. R. Gil, K. Matyjaszewski, Macromolecular Chemistry and Physics 2008, 209, 32.

[60] L. Mueller, W. Jakubowski, K. Matyjaszewski, J. Pietrasik, P. Kwiatkowski, W. Chaladaj, J. Jurczak, European Polymer Journal 2011, 47, 730.
[61] W. Jakubowski, K. Min, K. Matyjaszewski, Macromolecules 2006, 39, 39.
[62] H. Li, Y. M. Zhang, M. Z. Xue, Y. G. Liu, Polymer Journal 2005, 37, 841.
[63] X. Huang, Z. Huang, J. Huang, Journal of Polymer Science Part A: Polymer Chemistry 2000, 38, 914.
[64] L. Costa, M. Avataneo, P. Bracco, V. Brunella, Polymer Degradation and Stability 2002, 77, 503.
[65] C. Y. Liang, S. Krimm, Journal of Polymer Science 1958, 27, 241.
[66] J. R. Isasi, L. C. Cesteros, I. Katime, Macromolecules 1994, 27, 2200.
[67] E. Otsuka, S. Kudo, M. Sugiyama, A. Suzuki, Journal of Polymer Science Part B: Polymer Physics 2011, 49, 96.
[68] K. E. Strawhecker, E. Manias, Chemistry of Materials 2000, 12, 2943.
[69] J. E. K. Schawe, Thermochimica Acta 2015, 603, 128.
[70] D. Christie, R. A. Register, R. D. Priestley, ACS Central Science 2018, 4, 504.
[71] A. Hasimi, A. Stavropoulou, K. G. Papadokostaki, M. Sanopoulou, European Polymer Journal 2008, 44, 4098.
[72] Data from DeltaMem AG. Contact directly DeltaMem AG.
[73] A. Angelini, C. Fodor, L. Leva, A. Car, I. A. Dinu, W. Yave, W. Meier, Journal of Applied Polymer Science 2022, 139, 51562.
[74] F. S. Bates, G. H. Fredrickson, Annual Review of Physical Chemistry 1990, 41, 525.
[75] R. D. Groot, T. J. Madden, The Journal of Chemical Physics 1998, 108, 8713.
[76] S. P. Nunes, R. Sougrat, B. Hooghan, D. H. Anjum, A. R. Behzad, L. Zhao, N. Pradeep, I. Pinnau, U. Vainio, K.-V. Peinemann, Macromolecules 2010, 43, 8079.
[77] H. Ahn, S. Park, S.-W. Kim, P. J. Yoo, D. Y. Ryu, T. P. Russell, ACS Nano 2014, 8, 11745.
[78] T. Bucher, V. Filiz, C. Abetz, V. Abetz, Membranes 2018, 8, 57.
[79] A. Debuigne, J.-R. Caille, N. Willet, R. Jérôme, Macromolecules 2005, 38, 9488.
[80] G.-H. Li, C.-G. Cho, Colloid and Polymer Science 2005, 283, 946.
[81] P. W. Majewski, K. G. Yager, Nano Letters 2015, 15, 5221.
[82] P. W. Majewski, K. G. Yager, Journal of Physics: Condensed Matter 2016, 28, 403002.

The table of contents entry should be 50–60 words long and should be written in the present tense. The text should be different from the abstract text.

ToC

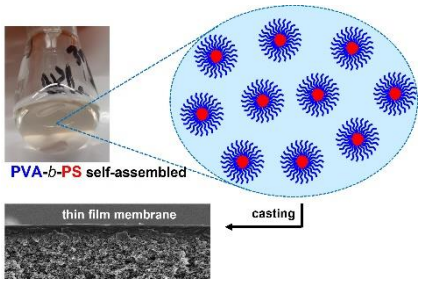

Supporting Information for

Amphiphilic poly(vinyl alcohol) membranes leaving out chemical cross-linkers: Design, synthesis, and function of tailor-made poly(vinyl alcohol)-*b*-poly(styrene) copolymers

Alessandro Angelini[a], Anja Car[a], Ionel Adrian Dinu[a], Luigi Leva[b] and Wilfredo Yave[b]

(a) Department of Chemistry, University of Basel, Mattenstrasse 24a, BPR 1096, 4058 Basel, Switzerland

(b) Research and Development Department, DeltaMem AG, Hegenheimermattweg 125, 4123 Allschwil, Switzerland

Synthesis of polystyrene macro precursor:
Benzyl bromide solution in anisole (0.043 mol.L-1, 40.21 mL, 1.72 mmol, 1 eq.) and tinII 2-ethylhexanoate solution in anisole (Sn(EH)2, 0.086 mol.L-1, 41.16 mL, 3.44 mmol, 2 eq.) were separately purged with argon for 90 min. In a Schlenk flask, equipped with a stirring bar, styrene (100 mL, 859 mmol, 500 eq.), copper(II) bromide (CuBr2, 38 mg, 0.172 mmol, 0.1 eq.), and tris[2-(dimethylamino)ethyl]amine (Me6TREN, 40 μL, 0.172 mmol, 0.1 eq.) were dissolved in anisole (20 mL) and purged with argon for 90 min. The initiator and reducing agent solutions were transferred to the Schlenk flask via a cannula. The polymerization was carried out in thermostated oil-bath at 90 °C for 2.5 h. Then, the flask was cooled to room temperature in an ice-cold water bath and the reaction was stopped by exposure to the air. The copper catalyst was removed by passing the solution over a column of neutral alumina oxide. The polymer was precipitated into cold methanol. The polymer was filtered and dried under vacuum at room temperature (white powder). 1H NMR (500 MHz, CDCl3, 295 K, δ, ppm): 7.24–6.30 (m, 5H, –CH2–CH(C6H5)–), 4.59–4.35 (m, 1H, –CH2–CH(C6H5)–Br), 2.13–1.68 (m, 1H, –CH2–CH(C6H5)–), 1.65–1.24 (m, 2H, –CH2–CH(C6H5)–).

Synthesis of PS-N_3:
PS-Br, 11 g, 1.1 mmol, 1 eq.) was dissolved in 50 mL of DMF in a round-bottom flask. Sodium azide (NaN3, 3.97 g, 60 mmol, 50 eq.) was added to the solution. The reaction was stirred overnight at room temperature. The reaction was poured into 500 mL of water and the

polymer was filtered and dried under vacuum (white powder). 1H NMR (500 MHz, CDCl3, 295 K, δ, ppm): 7.24–6.30 (m, 5H, –CH2–CH(C6H5)–), 4.04–3.83 (m, 1H, –CH2–CH(C6H5)–N3), 2.13–1.68 (m, 1H, –CH2–CH(C6H5)–), 1.65–1.24 (m, 2H, –CH2–CH(C6H5)–).

Synthesis of PS-CTA:

O-Ethyl S-(prop-2-yn-1-yl) carbonodithioate was synthesized according to literature procedures.200 PS-N3 (10 g, 1 mmol, 1 eq.), O-Ethyl S-(prop-2-yn-1-yl) carbonodithioate (0.33 mL, 2 mmol, 2 eq.), PMDETA (0.383 mL, 2 mmol, 2 eq.) were dissolved in THF (104 mL). The mixture was purged with argon for 90 min and subsequently copper(I) bromide (CuBr, 0.26 g, 2 mmol, 2 eq.) was added to the mixture under argon atmosphere. The reaction was stirred overnight at RT. The copper catalyst was removed by passing the solution over a column of neutral alumina oxide. The purified polymer was obtained by successive precipitations into methanol. The polymer was filtered and dried under vacuum (yellowish powder). 1H NMR (500 MHz, CDCl3, 295 K, δ, ppm): 7.24–6.30 (m, 5H, –CH2–CH(C6H5)–), 5.10–4.90 (m, 1H, –CH2–CH(C6H5)–triazole ring), 4.72–4.59 (2H, –CH2−S–), 4.54–4.32 (2H, –O−CH2), 1.65–1.24 (m, 2H, –CH2–CH(C6H5)–).

Synthesis of PS-*b*-PVAc:

In a dried and nitrogen purged polymerization Schlenk-flask, vinyl acetate (VAc, 65 mL, 0.682 mol, 3000 eq.), PS-CTA (2.5 g, 0.23 mmol, 1 eq.), azobisisobutyronitrile solution in THF (AIBN, 0.05 mol.L-1, 0.57 mL, 0.028 mmol, 0.125 eq.) and THF (16.9 mL) were added. After purging with nitrogen by cooling the flask in an ice bath, the tube was backfilled with argon, sealed, placed in an oil bath at 70 °C and removed after 17 h. The tube was subsequently cooled with liquid nitrogen to cease the reaction. The reaction mixture was diluted with THF and subsequently precipitated into 500 mL of methanol/water (1 : 1, v/v). The polymer was filtrated and dried overnight under vacuum (white powder). 1H NMR (500 MHz, CDCl3, 295 K, δ, ppm): 7.24–6.30 (m, 5H, –CH2–CH(C6H5)–)), 5.10–4.90 (1H, –CH2–CH(O–C(CH3)=O)–), 2.10–2.00 (3H, aliphatic protons of PVAc), 1.65–1.24 (m, 2H, –CH2–CH(C6H5)–).

Synthesis of PS-*b*-PVA:

The block polymer (PS-b-PVAc, 136 kDa, 29 g, 2 mmol, 1 eq.) was dissolved in 215 mL of THF. Potassium hydroxide solution in methanol (1.78 mol.L-1, 220 mmol) was prepared and

144 mL were added to the polymer solution (THF/MeOH, 1.5:1, v/v). The obtained mixture was stirred at room temperature for 4 h. The precipitated product was filtrated, washed with methanol and dried under vacuum a white powder. 1H NMR (500 MHz, DMSO-d6, 295 K, δ, ppm): 7.24–6.30 (m, 5H, –CH2–CH(C6H5)–), 4.68–4.24(3H, –CH2–CH(OH), 3.84 (1H, –CH2–CH(OH)–), 1.65–1.24 (aliphatic protons of PVA and PS).

Table S1. Summary of articles reporting copolymers of PVA and PS (including those as PVAc instead of PVA because they can be hydrolyzed to obtain PVA)

Year	Copolymer	Mn (NMR or GPC)	PD	PVA/PS ratio	Journal
1960	PS-b-PVA	17-44 kDa PS (η)	n.a.	0,3-1,2	Die Macromolekulare Chemie 36 (1960) 93
1966	PVA-alt-PS	n.a.	n.a.	0,9-1,1	J Polym Scie B: Polym Letters 4 (1966) 187
1978	PVAc-PS	8-50 kDa	1.3-5,1	0,2-0,3	J Polym Scie: Polym Chem Edition 16 (1978) 2527
1993	PS-b-PVAc	PS: 9-16 kDa	n.a.	0,3-1,2	J Appl Polym Scie 48 (1993) 425
1995	PS-g-PVA	22k Da (PS)	xx	0,9-10	Polymer 36 (1995) 4515
1997	PVA-b-PS-b-PVA	5-15k Da	PS: 1,5	0,05-0,3	J Appl Polym Scie 63 (1997) 849
1998	PS-b-PVA	26-34k Da	>2	1,3-4,0	J Polym Sci A: PolymChem 36 (1998) 109
1999	PVA-g-PS	8-23k Da	xx	1,4-23	Langmuir 15 (1999) 3197
1999	PVAc-b-PS	8-99k Da	1,4-2,2	0,2-1,2	Macromolecules 32 (1999) 7023
2000	PVAc-b-PS	-	1,2-1,4	-	Macromol: Chem Phys 201 (2000) 1189
2002	PVA-b-PS	5-15k Da	1,3-1,4	0,4-0,5	Macromol Res 10 (2002) 339
2003	PVA-PmAS	1,5-1,9k Da	1,8-2,2	0,1-1,0	J Membr Scie 216 (2003) 107
2005	PVA-b-PS	5-7k Da	1,2-1,5	3,0-1,0	Colloid Polym Scie 283 (2005) 946
2005	PVA-b-PS	20k Da	1,3-1,3	0,2-0,2	Macromolecules 38 (2005) 9488
2005	PVA-b-PS	5-30k Da	1,3-1,5	1,6-1,6	Polym J. 37 (2005) 841
2006	PVA-b-PS	12-45k Da	1,1-1,2	0,5-4,0	Chemm Comm (2006) 5051
2006	PVA-b-PS	9-15k Da	xx	0,4-0,8	Macromol Res 14 (2006) 504
2007	PVA-b-PS	30-45k Da	1,5-1,7	0,3-0,5	J Polym Sci A: PolymChem 45 (2007) 81
2008	PVAc-b-PS	-	1,25	-	Chemm Comm 42 (2008) 5336
2008	PVA-b-PS	2-5k Da	xx	0,7-2,5	Korean J Chem Eng 25 (2008) 1444
2008	PVAc-b-PS	12-72k Da	1,4-1,5		Macromolecules 41 (2008) 7339
2010	PVA-b-PS	15-25k Da	1,3-1,5	0,5-1,5	Macromolecules 43 (2010) 2184
2010	PVA-b-PS				Polymer 51 (2010) 3083
2015	PVAc-b-PS				Macromolecules 48 (2015) 6832
2017	PVAc-b-PS	31-64k Da	1,3-1,5		Polym Chem 8 (2017) 5918
2018	PS-b-PVA	9-15k Da	1,3-1,4	0,5-1,3	Polym Chem 9 (2018) 4243
2018	PS-b-PVA	43 kDa	1,4	10,0-10,1	J Polym Sci A: PolymChem 56 (2018) 2445
2018	PVA-b-PS	5-42k Da	1,2	0,3-2,7	Polymer 139 (2018) 68
2022	PVA-g-PS	125k Da PVA		65-330	Ind Eng Chem Res 61 (2022) 5797
2022	PVA-b-PS	5-15k Da	2,0-2,6	0,2-0,6	Polymer source
2022	PVA-b-PS	5-94 kDa	1,5-2,0	0,1-0,6	Polymer source

Table S2. PS-Br homopolymers obtained with different formulations and PS-*b*-PVAc

Sample	Mn [g/mol]	Conversion [%]	PD
PS_{57}	5900	11	1.11
PS_{100}	10400	20	1.08
PS_{57}-*b*-$PVAc_{225}$	25000	56	1.52
PS_{57}-*b*-$PVAc_{587}$	32000	59	1.55

Table S3. Solubility test of copolymers in different solvents

Sample	solvent	Result
PVA-63, PVA-81	acetone	insoluble
	acetonitrile	insoluble
	(MeOH, EtOH and IPA)	insoluble
	CHCl3	insoluble
	DMAc	soluble (with heat)
	dioxane	insoluble
	DMF	insoluble
	DMSO	soluble
	ethyl acetate	insoluble
	THF	insoluble
	toluene	insoluble
	water	insoluble
PVA-68, PVA-79, PVA-87, PVA-92	acetone	insoluble
	acetonitrile	insoluble
	(MeOH, EtOH and IPA)	insoluble
	CHCl3	insoluble
	DMAc	poorly soluble (with heat)
	dioxane	insoluble
	DMF	insoluble
	DMSO	soluble
	ethyl acetate	insoluble
	THF	insoluble
	toluene	insoluble
	water	insoluble

Table S4. Crystallinity and melting point of PVA block in dense films

Sample	Crystallinity [%]	T_m^{PVA} [°C]
PVA-68	39.3	230.3
PVA-79	10.5	217.7
PVA-87	20.3	222.0
PVA-92	24.6	223.8
PVA-100	50.6	231.0

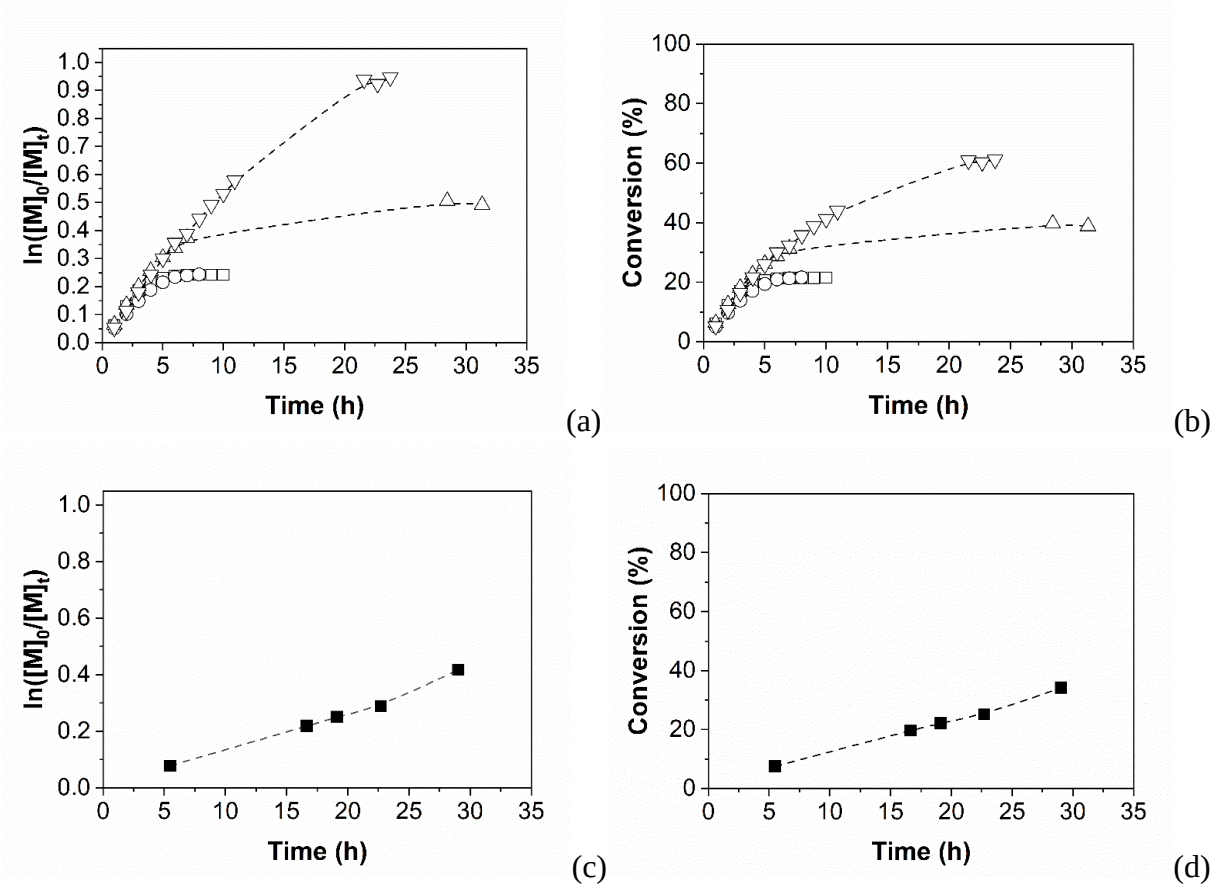

Figure S1. (a) and (b), kinetic study of PS synthesis by ARGET-ATRP (square data: according to Altintas et al, circle data: reduced initiator and catalyst, triangle up data: increased reducing agent x2, and triangle down data: increased reducing agent x4), and (c) and (d), polymer chain extension by VAc polymerization via RAFT

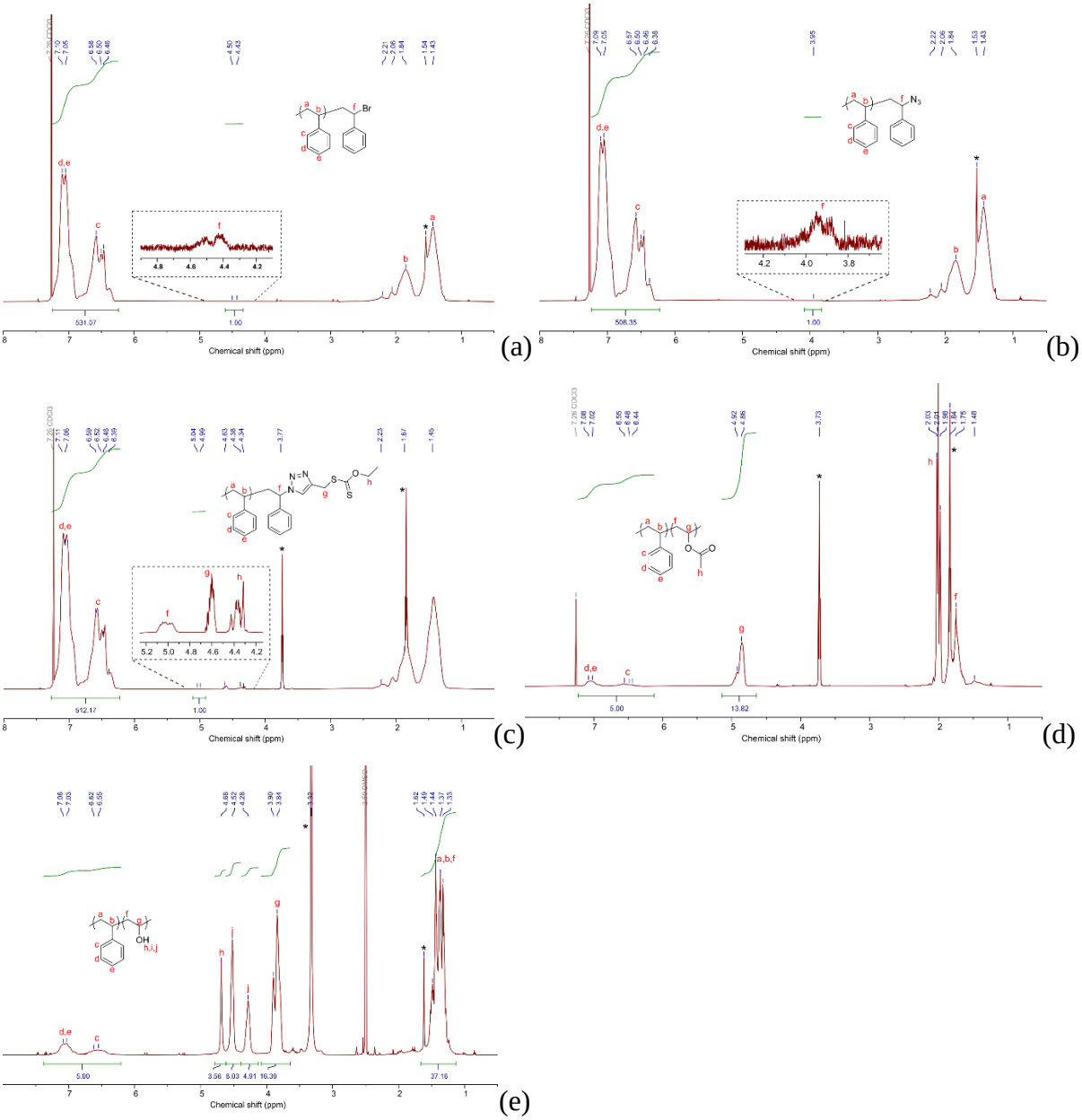

Figure S2. ^{1}H NMR spectra corresponding to PS-Br (a), PS-N_3 (b), PS-CTA (c), PS-*b*-PVAc (d) in CDCl3, and PS-*b*-PVA (e) copolymer in DMSO-d6 at room temperature (residual solvent is marked with an asterisk)

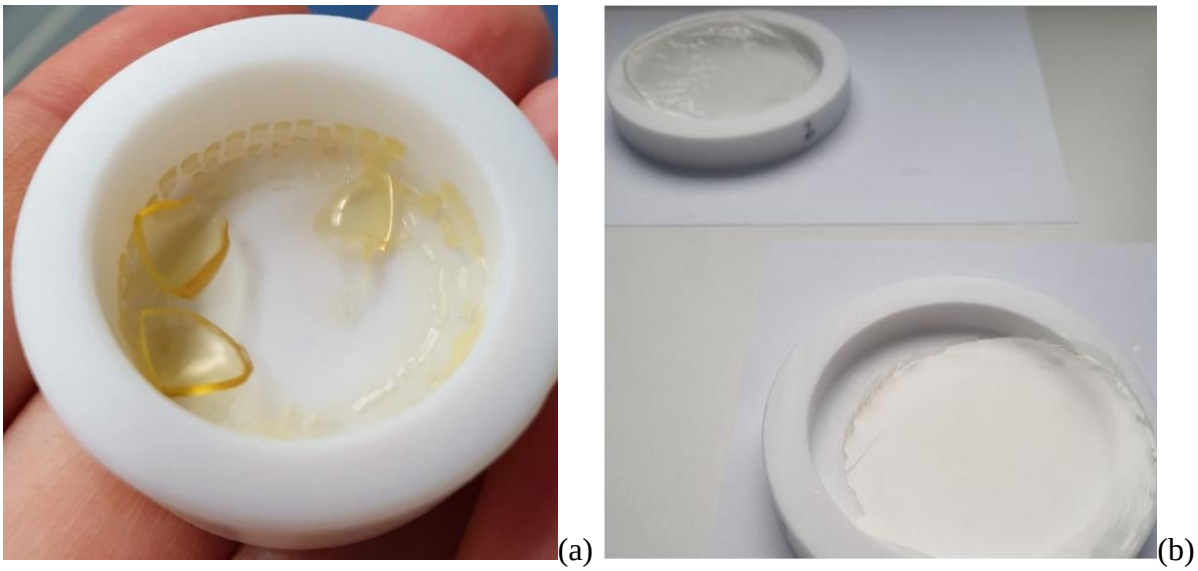

Figure S3. Pictures of self-standing dense films prepared from copolymers with low Mn (a) and copolymers with high Mn (b)

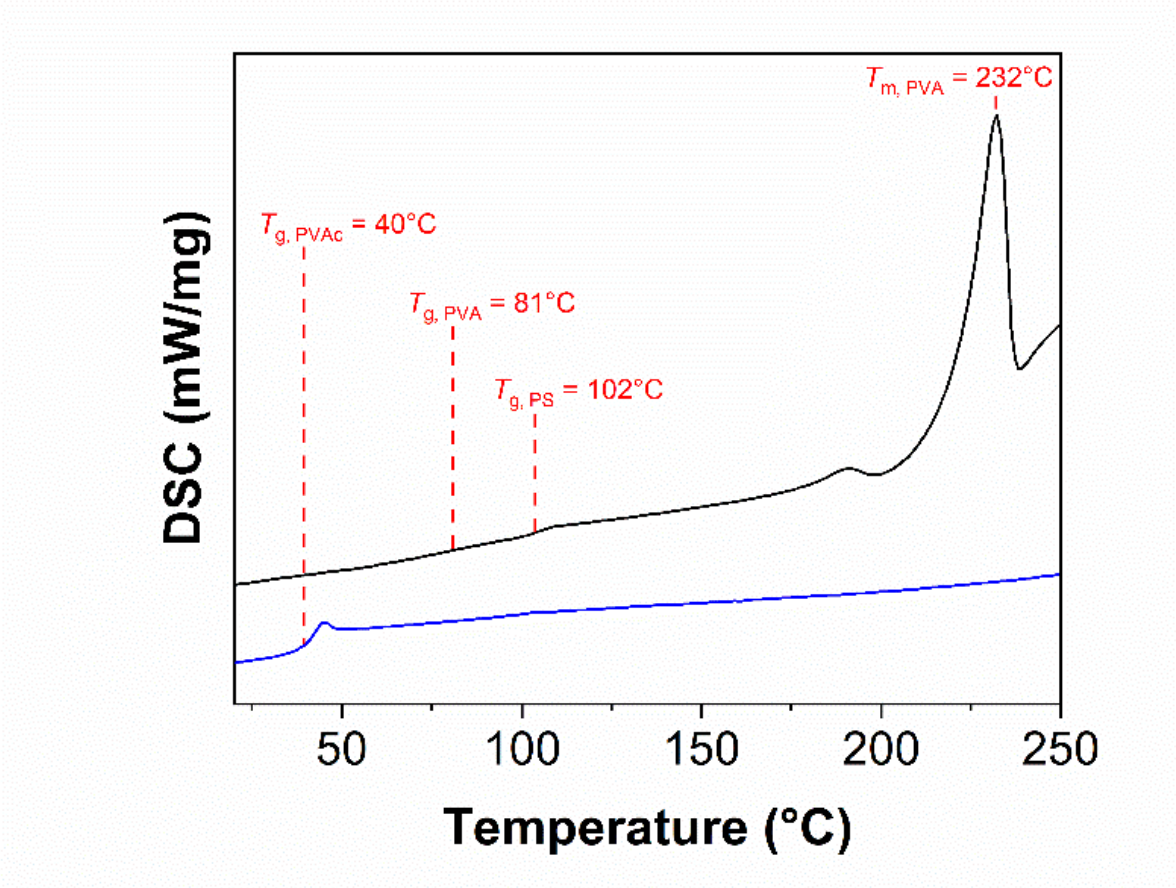

Figure S4. DSC thermograms (second heating scans, heating rate = 10 K min^{-1}) corresponding to PS-*b*-PVAc (blue), and after hydrolysis to obtain PS-*b*-PVA (black)

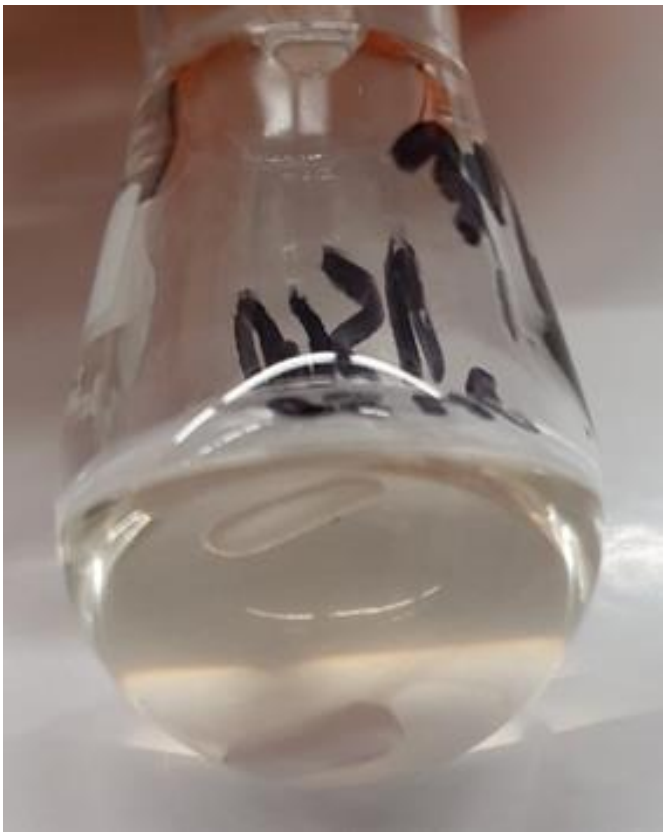

Figure S5. Picture of self-assembled micelle solution obtained by switching the solvent (from DMSO to water) by dialysis

Figure S6. Picture of the self-standing thin film obtained from the self-assembled micelle solution (difficult to handle)

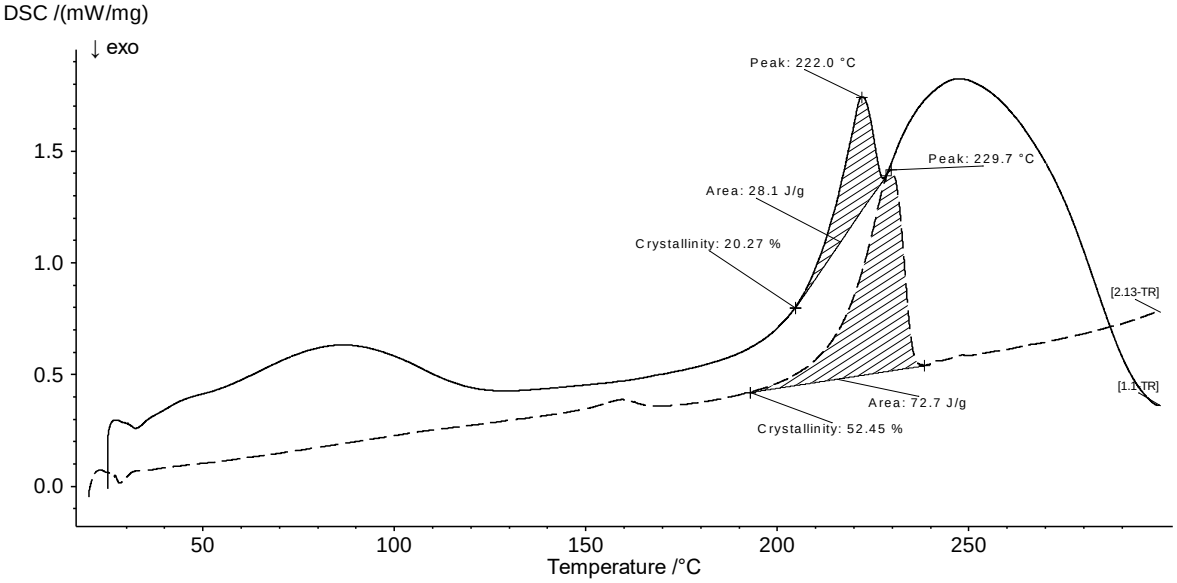

Figure S7. DSC thermograms corresponding to PVA-87 film before and after thermal annealing at 145 °C. As seen, the crystallinity of PVA block increases from 20.27% to 52.45% (the bump after the melting of PVA in the sample before the annealing is due to the polymer degradation, since the heating cycle reaches 250°C)

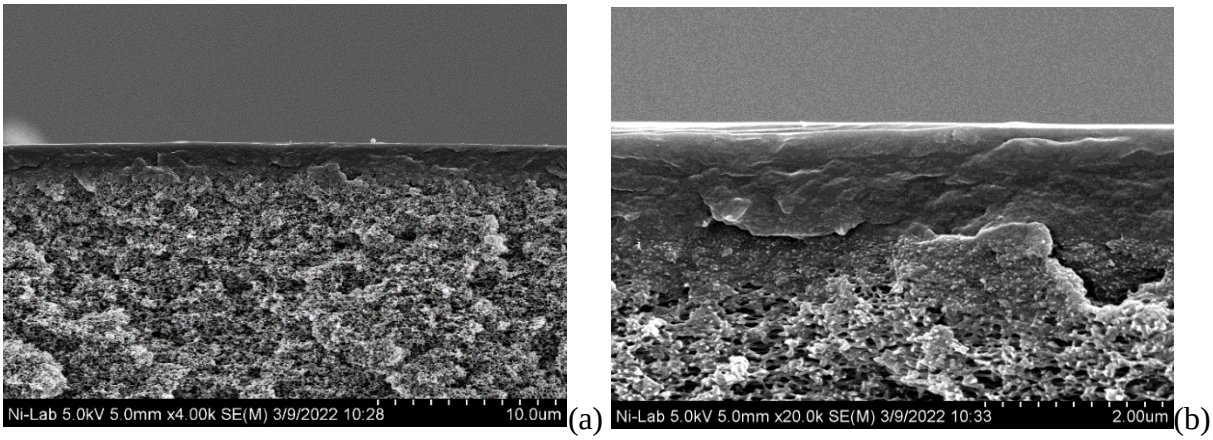

Figure S8. SEM micrographs of thin film membrane on porous substrate, sample PVA-87